11/30/99 RF

Repository & Drift Outline Coordinates

A request through Chad Glenn was made last August for DOE to provide the spatial coordinates of the current repository and drift outlines including the coordinate projection used by DOE. This was received 17 Nov 99 as and arcinfo export file (e00 file) with the coordinates (including elevations) projected as State Plane NAD27 (~~meters~~) feet. RF 2/7/00

Ron Martin converted the e00 to arcinfo shape files and stored them on vulcan: /project/gis/pub2/doe/design1099/*

I re-projected the shape files on bubo using ArcView V.3.1 's Project! extension

Matthew Knop GIS coordinator, Yucca Mtn Project
Matt_Knop@ymp.gov (702) 295-4808
is the person I directly dealt with throughout the fall as this data package was being developed. Mark Tynan approved its release to NRC and the center

This data set will be used to create the new subareas. It also serves the purpose in the TPA code of identifying the absolute data sets (spatial data) with known projection (Previously UTM NAD27 & NAD83 may have been mixed). The near-field and infiltration subareas were re-aligned by Rob Rice to be consistent; he didn't know which one was correctly matched with the topographic DEM spatial data (which I determined to be in UTM NAD27 (m)).

The rock mechanics people came to me (thanks to Sita Kanta) with a request for the outline of the drifts in ascii format. The following page contains that data (and a sigmaplot figure to check my data extraction). The next page (p.60) contains the DOE-provided pdf figure of what was contained in the data package. I extracted the coordinates by reading cursor positions in the UTM NAD27 projected data in ArcView version 3.1 (the data is stored in ArcView in its original coordinates of State Plane, so automatic exporting was not useful

unless I re-projected the exported files, say in arcinfo; the manual way seemed faster because I considered it more reliable).

bubo: D:\AVData\Repository* → The shape files
bubo: D:\AVData\Repository\Drift-ASCII\drift1.txt (main)
\drift2.txt (eastern block)
\drift.jnb (sigma plot)

EDA-II Drift Layout, DOE Preliminary 21Oct99

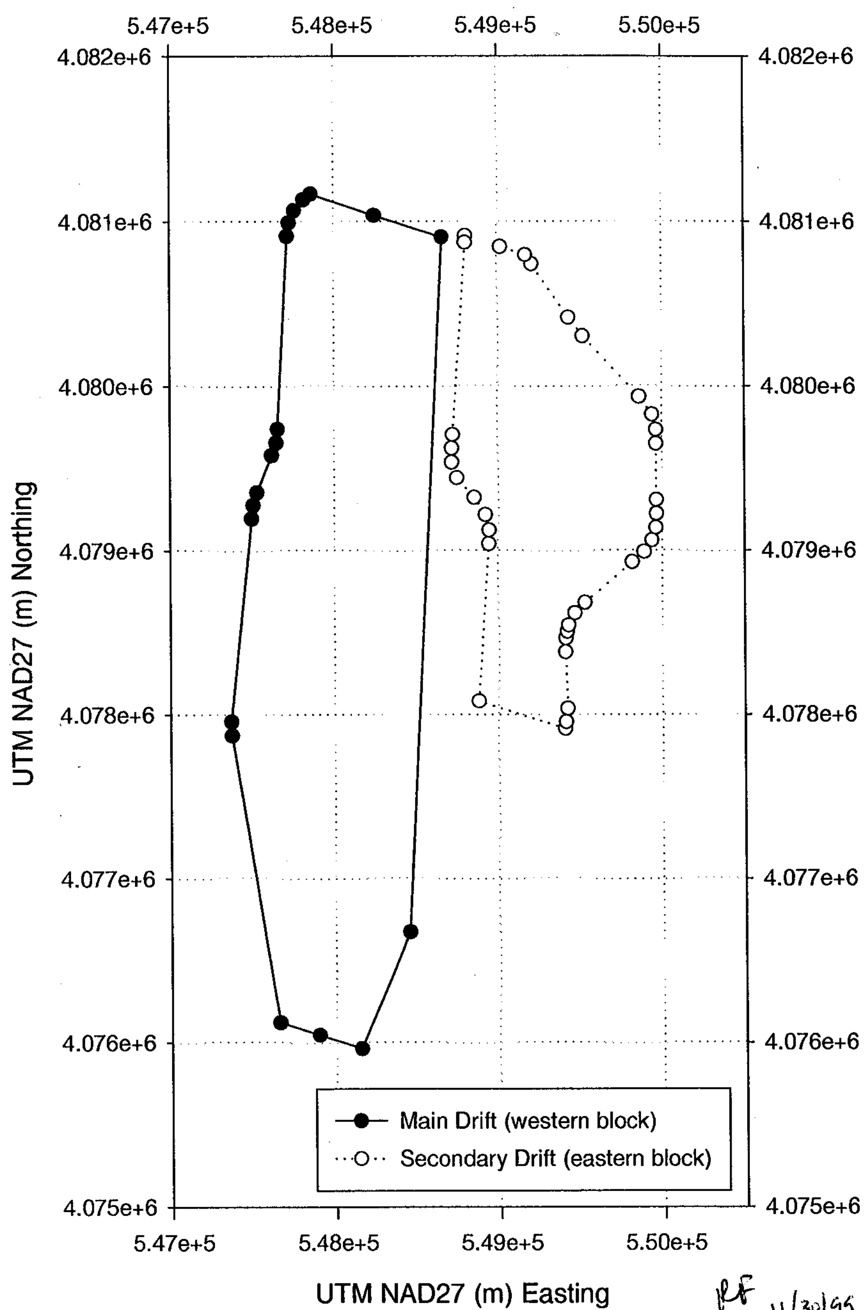

RF 11/30/99

drift1.txt (main block) RF 11/30/99

547864.13	4081164.96
547817.56	4081131.62
547760.36	4081064.93
547727.87	4080990.32
547716.90	4080908.79
547654.61	4079738.09
547645.27	4079656.06
547618.62	4079579.57
547528.18	4079353.45
547504.18	4079276.11
547495.21	4079193.94
547369.71	4077958.50
547372.63	4077872.50
547655.97	4076123.07
547897.79	4076045.46
548155.70	4075962.63
548455.00	4076674.51
548664.55	4080902.19
548251.91	4081034.69
547864.13	4081164.96

drift2.txt (eastern, secondary block) RF 11/30/99

548807.72	4080912.45
548804.96	4080870.81
548727.51	4079704.98
548721.97	4079621.72
548721.83	4079536.71
548751.62	4079442.10
548855.72	4079323.62
548923.81	4079216.71
548944.87	4079124.92
548942.74	4079040.54
548879.13	4078082.90
549401.09	4077915.32
549406.86	4077955.99
549418.37	4078037.35
549406.76	4078381.28
549407.20	4078466.16
549416.77	4078505.62
549426.34	4078545.08
549465.10	4078617.89
549526.53	4078683.01
549818.25	4078929.53
549888.86	4078991.92
549936.52	4079061.66
549961.06	4079138.84
549964.84	4079222.67
549964.53	4079307.82
549963.35	4079648.40
549962.52	4079733.71
549940.99	4079825.66
549862.03	4079936.08
549519.01	4080301.36
549430.68	4080414.75
549208.92	4080741.11
549171.91	4080795.49
549019.29	4080844.51
548807.72	4080912.45

RF
11/30/99

bubo: D:\AVData\Repository\repository.apr is the ArcView project file that contains the DOE-supplied GIS data. The figure below is the DOE-supplied file: ymp99054-0.pdf in the same directory.

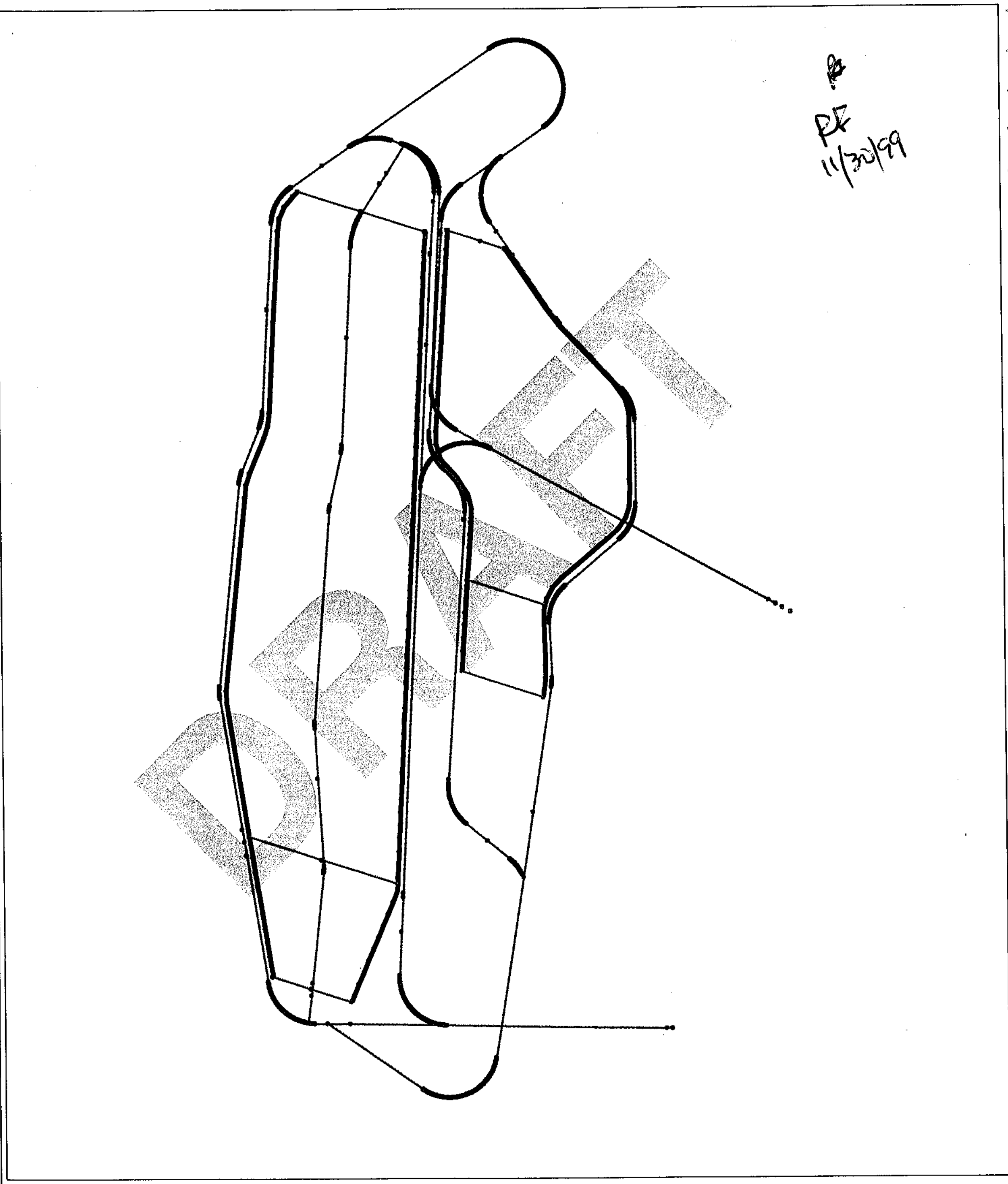

EDA-II Layout
Proposed Repository Outline and Projected Drifts

Legend
Repository Layout
Projected Drift Boundaries
Points with Elevation

Yucca Mountain Site Characterization Project

Map compiled by M&O/CRWMS/TDM/GI on October 21, 1999.
This data is preliminary and has not been submitted to the TDMS.

Draft: YMP-99-054.0

Incorporation of AirPhoto-Interpreted Surficial Materials to Split Wash Grid

David Groeneveld spent the week of Nov 29 – Dec 3rd, 1999 at the center using Amit Armstrong's NT box and ArcView 3.1 to map out surficial materials above repository (including main drift area and 2ndary drift area to east of ESF. He recorded his work in his own scientific notebook (w/ assigned number from Mabrito/QA). Briefly, he used the ortho-rectified air photo (~1m² resolution) (D:\AVData\Dog*), his higher-resolution air photo's taken from his airplane, and our knowledge from field work in Split Wash and across the repository footprint.

The following pages contain the Split Wash portion of Groeneveld's work, the modifications I made to the KINEROS2 grid because of the surficial materials, and the re-numbering required by those changes:

bubo: D:\AVData\WatershedGrid\Grid\plane1.* and channel2.*
D:\AVData\Groen\surface.shp
surface.dbf
surface.shx

The changes to the grid were minimal: 3 elements were added and 2 lines of elements had their borders shifted. Re-numbering of the eastern half of the grid was required because of the addition of plane elements. Two channel lengths were also changed.

I also had to clean-up Groeneveld's mapping (Quality-control)
1. I deleted all "uk" (unknown) records because they were all overlain by other categories now.
2. I checked all polygons with areas less than 500 m² to see if they were mistakes, or overlain, or adjacent to similarly categorized areas. Areas were deleted or joined as necessary
3. Shifting of contacts where 2 areas overlain

See pages 62-67

12/27/99 RF

New Grid with Plane Element Numbers (numbers-planes.apr)

also see page 67

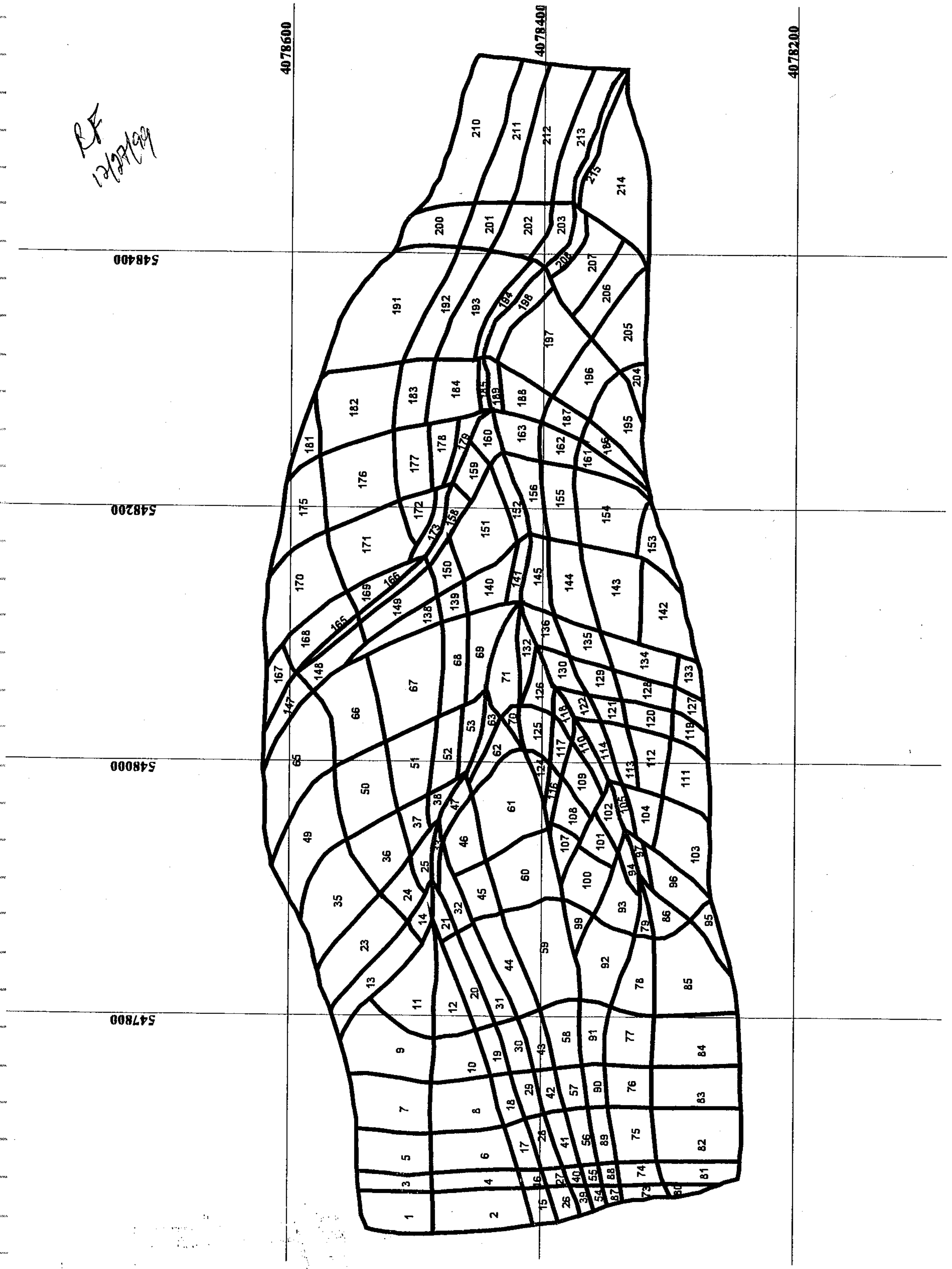

New Grid with Channel Element Numbers
Dubo: D:\AVData\WatershedGrid\numbers-channels.apr
RF 1/5/99

RF 12/27/99

also see page 67

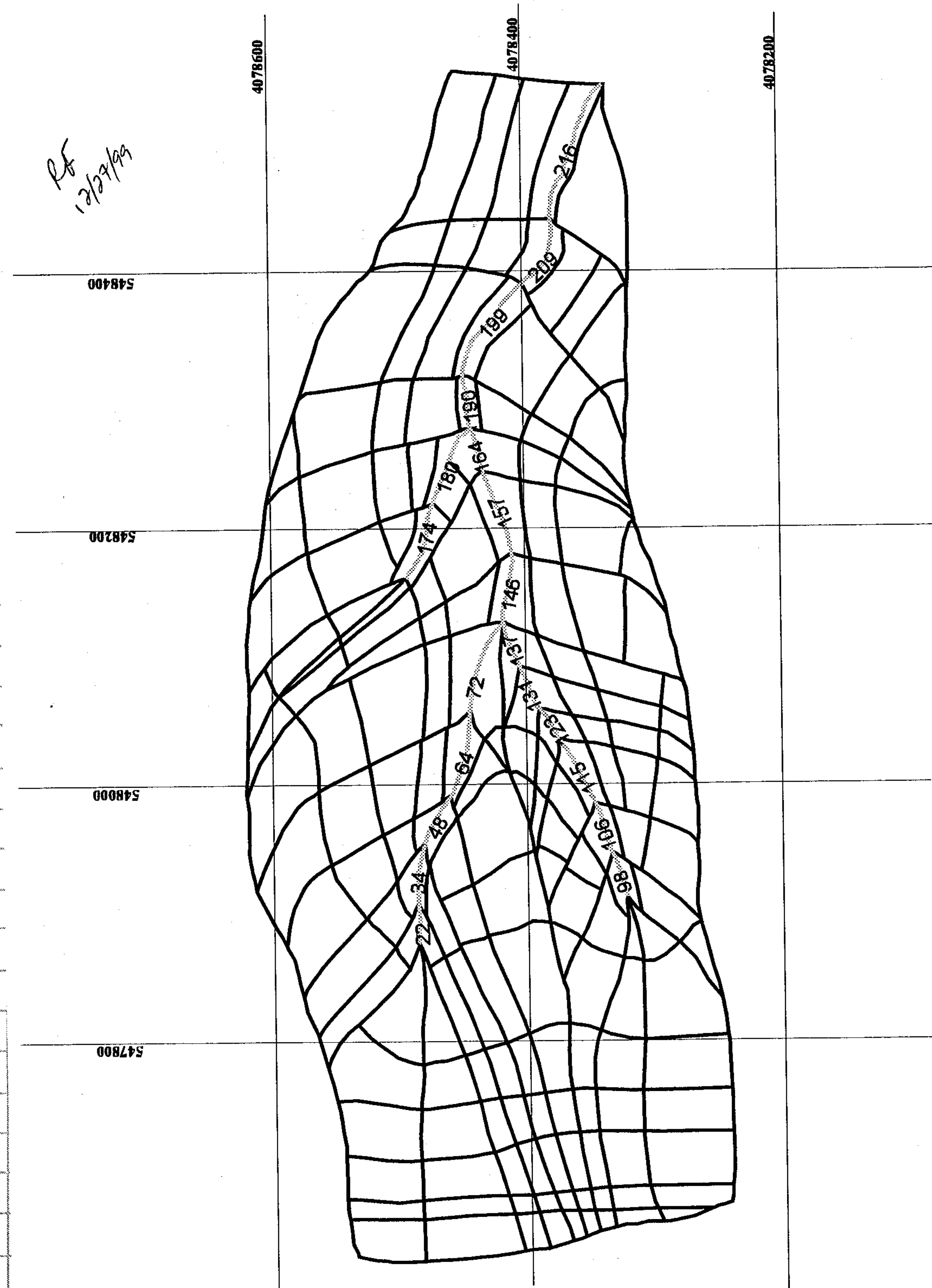

RF 12/27/99

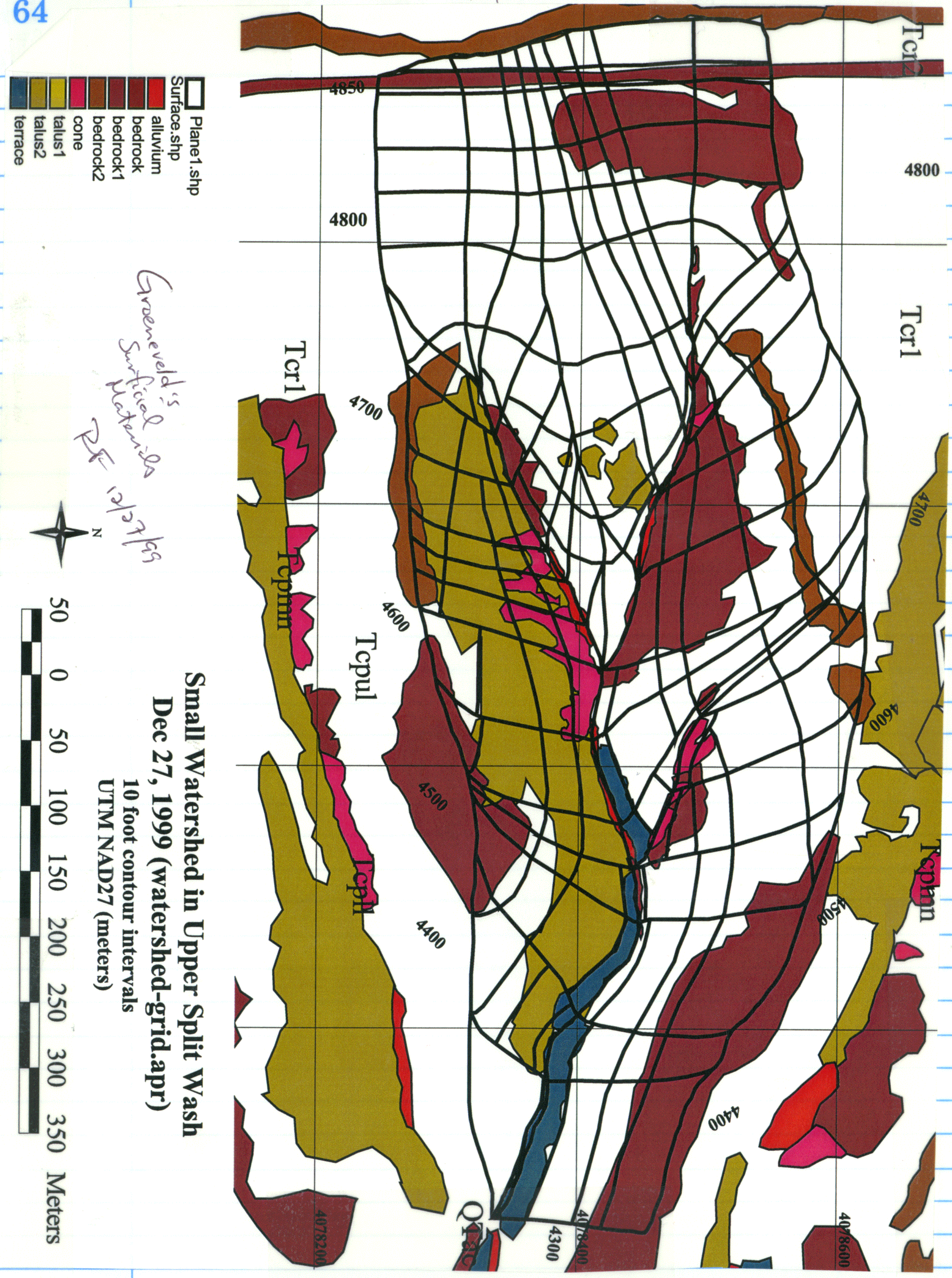

RF 12/27/99

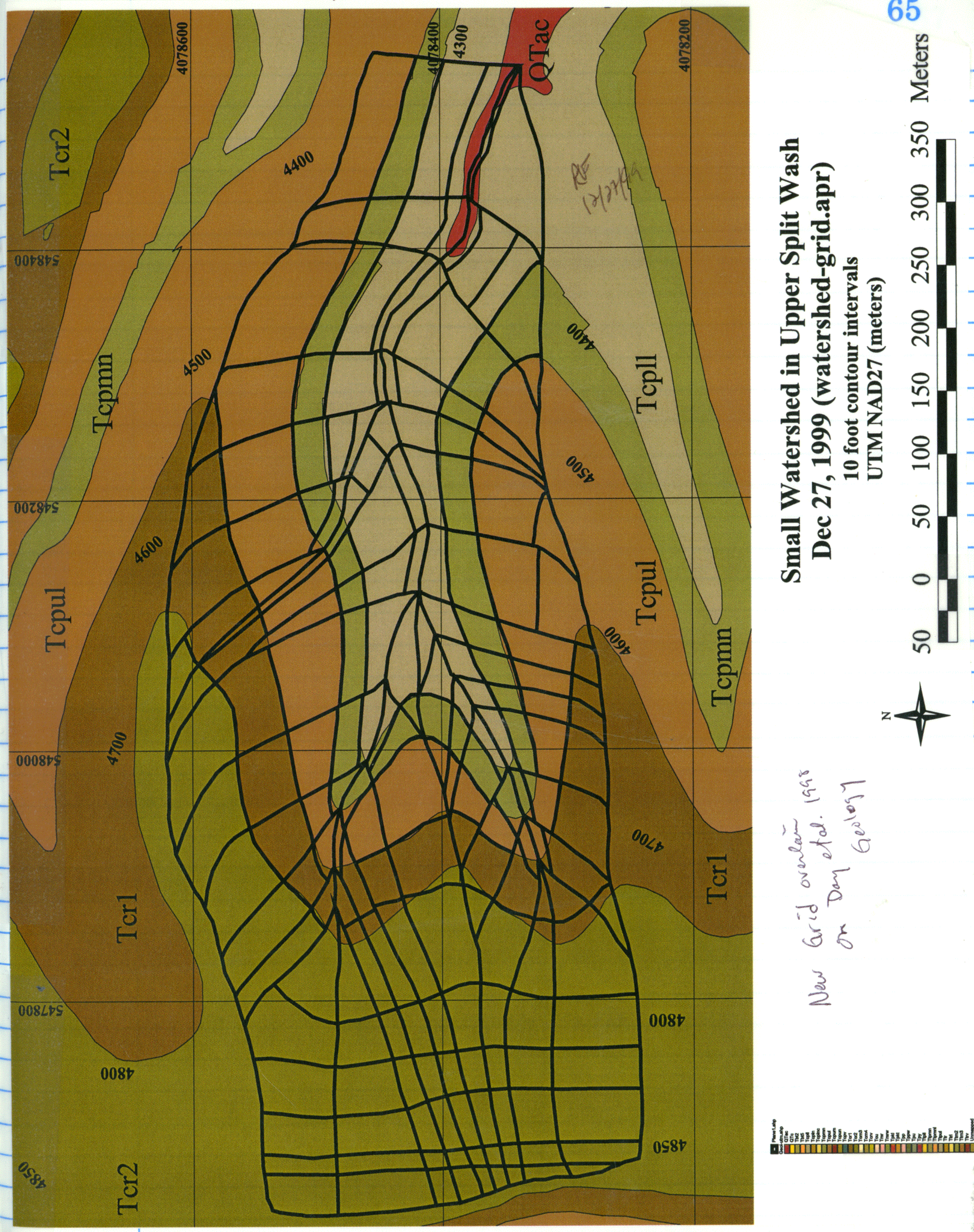

RF 12/27/99

New Grid overlain on 1m² ortho-rectified air photo

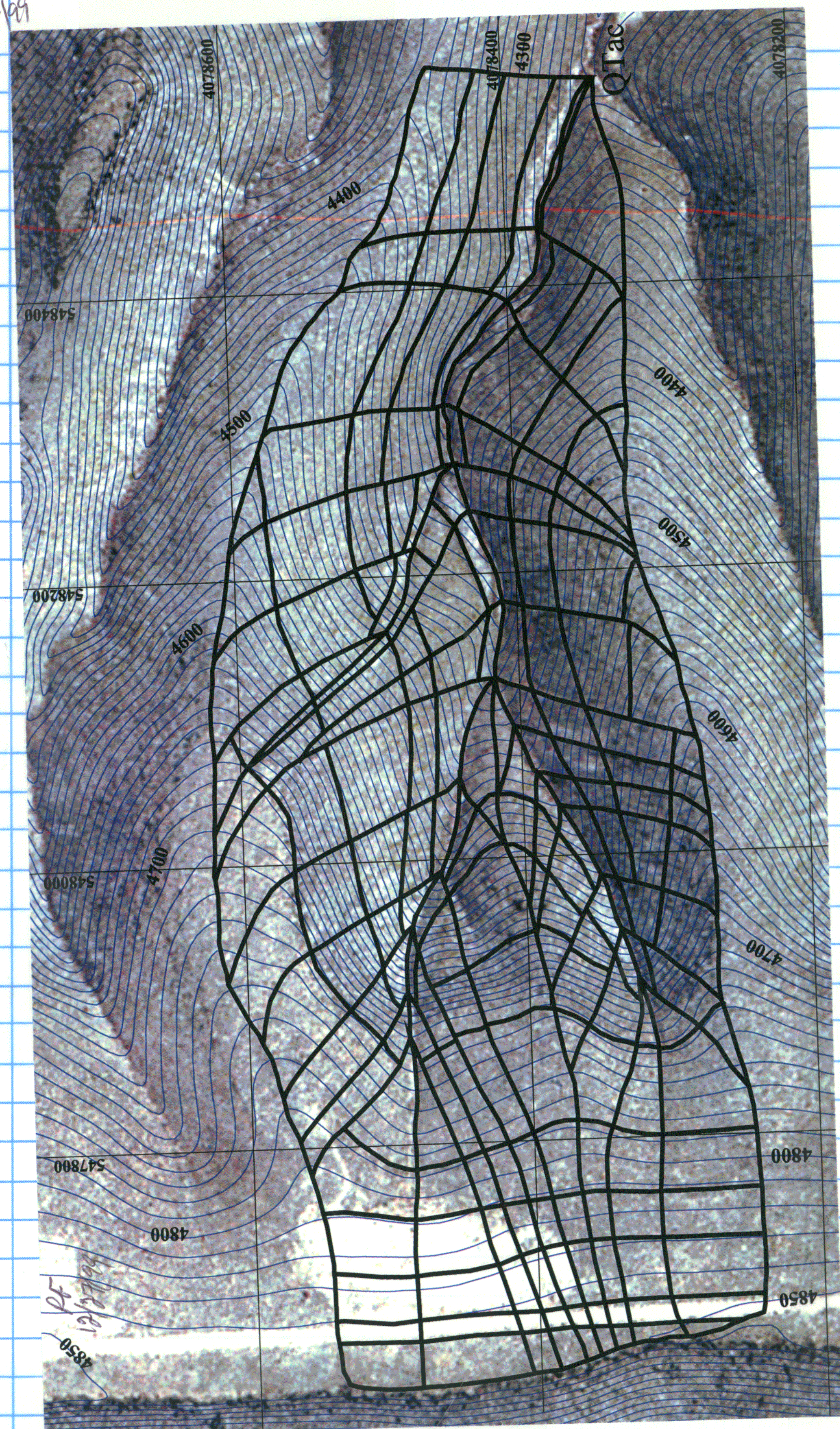

RF 12/27/99

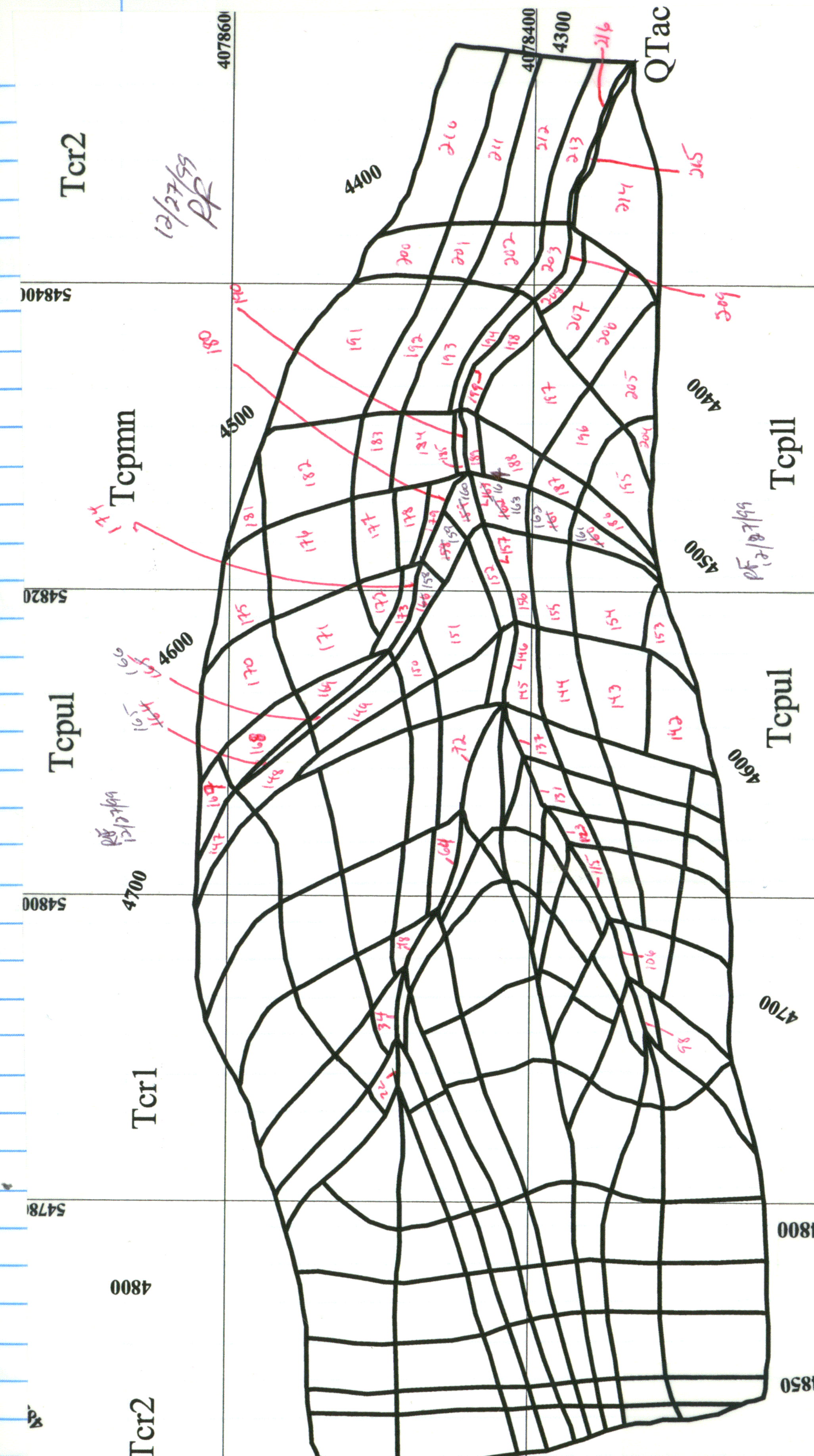

Re-numbering (changes) from old grid (see page 56)

Channel element numbers for western half of grid did not change – I just added them here for reference

To get numbers to scale in auto-label mode of ArcView 3.1, choose "Display overlapping labels", then after labeling
(1) select all labels & then Theme → Convert Labels
(2) Select any label then choose Window → Show Fonts and then choose desired font size
(see page 62 & 63 for re-numbered grids).

Summary of Areas, lengths, widths, & slopes of Elements

bubo: D:\Randy\Woolhiser\SplitWash\Grid\Detail1.xls

(1) Areas of each plane elements and channel length ~~was~~ calculated in ArcView were exported & then imported into EXCEL 97 SR-2 spreadsheet.

ArcView Table → [Shape].ReturnArea
"calculator" [Shape].Return Length
used to define
column entry

The spreadsheet uses the Area and the measured flow path length to calculate the representative width. KINEROS2 needs the length and width of each plane element and the length of each channel element. (As well as slope).

(2) Flow path in each element was approximated visually and the length was calculated using the measuring tool in ArcView.

(3) The slope for each plane and channel element was estimated by counting the contours between element endpoints along the flow path length. The elevation was entered into the spreadsheet and the slope was calculated using the measured flow path length. Between contours interpolation was used such that ~1 foot resolution was maintained in terms of accuracy.* RF 9/25/00

(4) Lengths, Widths and Slopes were entered into the KINEROS2 parameter input file "DET1A-mod.par"

(5) Woolhiser needs to input the soil thicknesses and Ks values

(6) Print out of spreadsheet on next page

* RF 9/25/00 In small section adjacent to streambed, measure length of flow line as perpendicular to the topo lines, and estimate elev change along this flow line. This gets the slope correct & it distributes water all along contact. Don't be confused by trying to estimate geometric length and width of the plane element.

Split Wash Watershed Grid (Jan 2000)
Areas of planes automatically calculated by ArcView
Lengths of flow path in each element measured as curvi-linear line
Elevation change is along the flow path.
Ks values now linked to top of column entry instead in each equation
Ks values from Flint et al. 1996, Table 2
QTac is alluvium/colluvium

RF 1/18/00

El #	Area m*2	Length, m	Width, m	Del.H, ft.	Slope
1	1786	33.1	54.0	4.0	0.037
3	841	13.9	60.5	1.3	0.029
5	1906	32.3	59.0	14.0	0.132
7	2594	43.5	59.6	18.0	0.126
9	3134	44.7	70.1	22.0	0.150
11	2398	86.6	27.7	67.0	0.236
2	2410	32.8	73.5	4.0	0.037
4	1027	14.6	70.3	1.4	0.029
6	1996	31.4	63.6	14.0	0.136
8	2093	40.4	51.8	18.0	0.136
10	1424	35.1	40.6	21.0	0.182
12	1431	92.0	15.6	68.0	0.225
13	1814	103.4	17.5	63.0	0.186
14	470	39.3	12.0	54.0	0.419
15	552	29.2	18.9	3.2	0.033
16	271	14.6	18.6	1.3	0.027
17	686	38.9	17.6	12.0	0.094
18	667	39.3	17.0	17.0	0.132
19	627	39.2	16.0	21.0	0.163
20	1166	75.9	15.4	53.0	0.213
21	455	45.5	10.0	64.0	0.429
22		30.4		49.0	0.491
23	2672	96.5	27.7	57.0	0.180
24	843	29.0	29.1	57.0	0.599
25	596	34.5	17.3	67.0	0.592
26	504	27.0	18.7	3.0	0.034
27	239	14.2	16.8	1.3	0.028
28	673	43.3	15.5	13.0	0.092
29	618	36.2	17.1	17.0	0.143
30	783	41.8	18.7	23.0	0.168
31	1287	79.6	16.2	54.0	0.207
32	793	55.1	14.4	87.0	0.481
33	265	52.5	5.0	89.0	0.517
34		47.9		79.0	0.503
35	3189	87.2	36.6	49.0	0.171
36	1870	43.8	42.7	86.0	0.598
37	677	24.4	27.7	49.0	0.612
38	424	30.0	14.1	49.0	0.498
39	255	22.8	11.2	2.3	0.031
40	204	15.8	12.9	1.4	0.027
41	689	45.1	15.3	13.0	0.088
42	559	33.7	16.6	17.0	0.154
43	795	45.6	17.4	24.0	0.160
44	1766	83.5	21.1	56.0	0.204
45	1028	40.3	25.5	68.0	0.514
46	1267	46.4	27.3	84.0	0.552
47	526	40.8	12.9	62.0	0.463
48		43.9		58.0	0.403
49	3213	105.3	30.5	58.0	0.168
50	2526	47.5	53.2	90.0	0.578
51	1927	36.3	53.1	68.0	0.571
52	1181	24.0	49.2	39.0	0.495
53	846	28.4	29.8	32.0	0.343
54	221	18.7	11.8	1.9	0.031
55	216	16.6	13.0	1.5	0.028
56	715	45.2	15.8	14.0	0.094
57	675	33.3	20.3	15.0	0.137
58	1311	51.6	25.4	25.0	0.148
59	3421	79.4	43.1	57.0	0.219
60	2586	50.3	51.4	87.0	0.527
61	3264	59.0	55.3	96.0	0.496
62	844	16.4	51.5	28.0	0.520
63	516	17.6	29.3	18.0	0.312
64		67.3		56.0	0.254
65	3877	102.7	37.8	57.0	0.169
66	2849	41.2	69.2	71.0	0.525

El #	Area m*2	Length, m	Width, m	Del.H, ft.	Slope
67	3846	57.5	66.9	97.0	0.514
68	1407	20.4	69.0	31.0	0.463
69	1596	27.8	57.4	40.0	0.439
70	262	34.2	7.7	47.0	0.419
71	1553	69.7	22.3	66.0	0.289
72		76.1		58.0	0.232
73	406	11.5	35.3	1.4	0.037
74	592	18.1	32.7	1.6	0.027
75	1424	43.1	33.0	13.0	0.092
76	1161	32.0	36.3	15.0	0.143
77	1581	41.8	37.8	24.0	0.175
78	1545	61.1	25.3	54.0	0.269
79	356	49.1	7.3	71.0	0.441
80	288	9.6	30.0	1.2	0.038
81	1066	17.5	60.9	1.6	0.028
82	2903	41.8	69.4	17.0	0.124
83	2312	32.3	71.6	17.0	0.160
84	2784	40.7	68.4	25.0	0.187
85	3663	67.9	53.9	52.0	0.233
86	768	53.5	14.4	73.0	0.416
87	197	14.9	13.2	1.6	0.033
88	258	17.6	14.7	1.6	0.028
89	685	44.4	15.4	14.0	0.096
90	569	33.9	16.8	17.0	0.153
91	1007	41.9	24.0	24.0	0.175
92	2153	55.5	38.8	52.0	0.286
93	1257	40.4	31.1	66.0	0.498
94	406	38.7	10.5	69.0	0.543
95	636	57.8	11.0	32.0	0.169
96	1384	52.0	26.6	83.0	0.487
97	355	40.2	8.8	68.0	0.516
98		36.8		60.0	0.497
99	508	38.8	13.1	35.0	0.275
100	1353	40.2	33.7	76.0	0.576
101	688	23.9	28.8	49.0	0.625
102	616	28.6	21.5	46.0	0.490
103	2180	59.8	36.5	85.0	0.433
104	906	25.7	35.3	55.0	0.652
105	367	24.5	15.0	33.0	0.411
106		41.1		50.0	0.371
107	584	41.9	13.9	75.0	0.546
108	812	27.6	29.4	50.0	0.552
109	931	31.0	30.0	57.0	0.560
110	534	17.8	30.0	24.0	0.411
111	1647	45.5	36.2	51.0	0.342
112	1246	28.2	44.2	46.0	0.497
113	836	20.6	40.6	43.0	0.636
114	677	31.5	21.5	37.0	0.358
115		57.2		51.0	0.272
116	344	48.8	7.0	75.0	0.468
117	494	35.6	13.9	59.0	0.505
118	361	21.7	16.6	25.0	0.351
119	595	37.5	15.9	37.0	0.301
120	788	39.1	20.2	58.0	0.452
121	452	24.1	18.8	41.0	0.519
122	463	25.3	18.3	34.0	0.410
123		27.2		19.0	0.213
124	377	38.3	9.8	58.0	0.462
125	896	36.8	24.3	54.0	0.447
126	752	40.3	18.7	42.0	0.318
127	491	31.6	15.5	31.0	0.299
128	904	46.0	19.7	64.0	0.424
129	777	33.7	23.1	56.0	0.506
130	712	36.8	19.3	41.0	0.340
131		37.2		29.0	0.238
132	619	72.4	8.5	75.0	0.316
133	531	27.4	19.4	26.0	0.289
134	1478	57.3	25.8	76.0	0.404
135	983	38.9	25.3	61.0	0.478
136	784	38.9	20.2	45.0	0.353
137		36.6		33.0	0.275
138	1029	86.3	11.9	137.0	0.484
139	511	22.8	22.4	30.0	0.401
140	1213	45.6	26.6	50.0	0.334
141	547	15.0	36.5	20.0	0.406

El #	Area m*2	Length, m	Width, m	Del.H, ft.	Slope
142	2288	60.2	38.0	58.0	0.294
143	2751	46.8	58.8	75.0	0.488
144	1903	40.7	46.8	63.0	0.472
145	1103	25.2	43.8	33.0	0.399
146		55.0		30.0	0.166
147	908	78.7	11.5	42.0	0.163
148	1044	59.2	17.6	89.0	0.458
149	1289	69.7	18.5	106.0	0.464
150	674	23.8	28.3	31.0	0.397
151	2582	61.3	42.1	69.0	0.343
152	872	23.8	36.6	19.0	0.243
153	975	52.9	18.4	33.0	0.190
154	2952	54.8	53.9	80.0	0.445
155	1556	26.3	59.2	47.0	0.545
156	1181	24.2	48.8	32.0	0.403
157		67.9		29.0	0.130
158	659	61.0	10.8	82.0	0.410
159	716	34.4	20.8	27.0	0.239
160	632	31.8	19.9	24.0	0.230
161	735	69.6	10.6	77.0	0.337
162	814	31.0	26.3	47.0	0.462
163	1067	40.2	26.5	46.0	0.349
164		34.9		14.0	0.122
165	282	64.5	4.4	93.0	0.439
166	468	70.7	6.6	104.0	0.448
167	776	60.9	12.7	40.0	0.200
168	1513	68.7	22.0	96.0	0.426
169	788	67.1	11.7	99.0	0.450
170	3429	85.9	39.9	95.0	0.337
171	3004	63.7	47.2	97.0	0.464
172	734	30.4	24.1	45.0	0.451
173	635	35.9	17.7	58.0	0.492
174		63.3		81.0	0.390
175	2112	57.4	36.8	58.0	0.308
176	3391	59.1	57.4	88.0	0.454
177	1507	29.4	51.3	45.0	0.467
178	890	20.5	43.4	29.0	0.431
179	588	23.8	24.7	22.0	0.282
180		66.8		54.0	0.246
181	739	34.0	21.7	24.0	0.215
182	3557	65.5	54.3	83.0	0.386
183	1346	26.8	50.2	40.0	0.455
184	1795	40.6	44.2	64.0	0.480
185	278	12.3	22.6	9.0	0.223
186	815	69.4	11.7	74.0	0.325
187	676	34.5	19.6	47.0	0.415
188	1132	39.7	28.5	50.0	0.384
189	407	18.0	22.6	15.0	0.254
190		41.9		18.0	0.131
191	5803	84.1	69.0	85.0	0.308
192	2048	21.6	94.8	33.0	0.466
193	2497	26.9	92.8	45.0	0.510
194	816	14.5	56.3	16.0	0.336
195	1808	81.7	22.1	85.0	0.317
196	1607	32.8	49.0	44.0	0.409
197	3354	56.3	59.6	64.0	0.346
198	1142	21.7	52.6	20.0	0.281
199		88.0		29.0	0.100
200	1500	57.1	26.3	58.0	0.310
201	1009	29.4	34.3	40.0	0.415
202	1469	36.9	39.8	50.0	0.413
203	921	28.1	32.8	28.0	0.304
204	464	45.9	10.1	45.0	0.299
205	2106	52.9	39.8	60.0	0.346
206	1654	21.9	75.5	31.0	0.431
207	1981	31.4	63.1	41.0	0.398
208	609	15.0	40.6	13.0	0.264
209		59.6		21.0	0.107
210	4298	53.7	80.0	48.0	0.272
211	2757	24.2	113.9	34.0	0.428
212	3381	31.1	108.7	46.0	0.451
213	2038	22.6	90.2	28.0	0.378
214	4408	82.1	53.7	85.0	0.316
215	698	18.0	38.8	11.0	0.186
216		114.6		40.0	0.106

Pages 70-105 taped in 9/28/00 RF

Watershed Modeling – Upper Split Wash **[4/10/00]**

Discretization and development of hydrologic input values for the Upper Split Wash watershed model was carried in concert with Dave Woolhiser as is already described in scientific notebook #362 Woolhiser and #294 Fedors. This section presents the model results used to create the deliverable report due out May 2000. See Woolhiser's notebook (#362) for the other figures and tables not described here.

Work was done using the NT box named bubo (pentium II, 450 MHz, 256 MBytes RAM) except that UNIX to DOS conversions of ascii files and running ITYM (TPA4.0) were done on the SUN Ultra named ds9.
ArcView version 3.1 and EXCEL 97 SR-2 work was done on the NT box.
Work is generally stored in: J:\AVData\WatershedGrid*
J:\AVData\Repository*
D:\Randy\Woolhiser\SplitWash*
The final figures are stored with the text of the report in:
J:\ShallowInfiltrationRpt\WatershedRpt*

Description of data elements for each figure in Upper Split Wash Watershed Modeling Report:

Figure 1-1: Location map of upper Split Wash.
The project file for this image is stored in J:\AVData\Repository.
J:\AVData\Repository\esf.shp .\ecrb.shp and .\drift.shp and associated files.
The ESF and drift outline are directly from DOE's/M&O's GISgroup (Matt Knop), the ECRB was digitized based on ECRB weekly progress maps and thus should be considered approximate (for the purpose of this figure that is okay). The basemap is from Ron Martin who got the digital orthoquads from the DOE. This is the northwest quarter of the Butte Quad:
J:\AVData\Doq\airfota_nw27.bip

Figure 2-1. Geometrical representation of KINEROS2. Created in Adobe Illustrator version 8.0.
J:\ShallowInfiltration\WatershedRpt\NewFigureNames\fig2-1.pdf

Figure 2-2. Geometrical representation of HILLS model. Created in Adobe Illustrator version 8.0.
J:\ShallowInfiltration\WatershedRpt\NewFigureNames\Fig2-2pdf

Figure 2-3. Location of hillslopes A, B, C.
ArcView project file: J:\AVData\Repository\hillslopeabc.apr
Used J:\AVData\Doq\airfota_nw27.bip as basemap and USGS topographic file J:\AVData\ctr_blk\topo10.shp; the source of doq file is described above (Figure 1-1). Topographic lines are from the Yucca Mountain geologic map by Day et al. (1998) USGS Misc Investigations Map I-2637 downloaded as an ArcInfo .e00 file from greenwood.cr.usgs.gov ftp site, converted to UTM NAD27 in ArcInfo, and stored in J:\AVData\Wday\Topo\topo*.
The locations of the hillslopes A, B, C were based on Woolhiser's choice of slopes to represent convergent, parallel, and divergent slopes as determined using the topographic contours.

Figure 2-5. Geometric representations of convergent, parallel, and divergent slopes.
Created in Adobe Illustrator 8.0 and saved as:
J:\ShallowInfiltration\WatershedRpt\NewFigureNames\Fig2-5_Hills-Kineros.pdf

Figure 2-12. Locations of other watersheds and meteorology stations.
ArcView project file is: J:\AVData\Repository\canyon-watersheds.apr
Topographic lines are from the Yucca Mountain geologic map by Day et al. (1998) USGS Misc Investigations Map I-2637 downloaded as an ArcInfo .e00 file from greenwood.cr.usgs.gov ftp site, converted to UTM NAD27 in ArcInfo, and stored in J:\AVData\Wday\Topo\topo*
Watershed outlines were digitized in ArcView using the topographic lines for accurate delineation and figure 6-15 of the Infiltration AMR (Rev. 00A) [Location of stream-gaging sites and ….] for qualitative agreement with the USGS watershed delineations.

Meteorologic Station locations plotted on this Figure 2-12 were obtained from the DOE web data page (TDMS, technical data management system) for the SAIC stations, and from the open-file report Flint and Davies (1997) USGS Open-File Report 96-462 [Meteorological Data for Water Years 1988-94 from Five Weather Stations at Yucca Mountain, Nevada.

Figure 3-1 to 3-5. Five figures created in ArcView with airphoto, topographic contours, Day et al. (1998, USGS Misc. Investigation Map I-2601) geology, and simple and detailed KINEROS2 grids [sources of all of this data has been previously described this notebook (#294), pages 16-39and 47-69]. The soil depths, instead of using the contoured data of Stothoff's soil model in the figure, uses the KINEROS2 input soil thicknesses directly. Woolhiser's visual estimation (sci ntbk #362) of contoured soil thicknesses (sci ntbk 294 page 51), the data used in the contouring is from Stothoff's soil model (sci ntbk #163). ArcView project files used to create these figures are:
J:\AVData\WatershedGrid\geol-dgrid.apr
J:\AVData\WatershedGrid\dgrid-channel-num.apr
J:\AVData\WatershedGrid\ dgrid-plane-numbers.apr
J:\AVData\WatershedGrid\geol&channels-numbers.apr
J:\AVData\WatershedGrid\numbers-planes.apr
J:\AVData\WatershedGrid\numbers-channels.apr
J:\AVData\WatershedGrid\soil-dgrid.apr
J:\AVData\WatershedGrid\soil-plane-numbers.apr
Stofhoff's soil thickness data (derived from his soil model) are stored in
J:\AVData\WatershedGrid\Soil-calculated\
J:\AVData\WatershedGrid\SoilMarch2000\ → revised soil depths used to tweak KINEROS soil thickness input values

Table 3-2. Hydraulic conductivity values and formation and lithologic unit names were taken from Flint et al. (1996) Conceptual and Numerical Model of Infiltration for the Yucca Mountain Area, Nevada, Draft USGS Water Resources Investigation Report. Table 2 of this Flint et al. report, last column (weighted K values) is the direct source.

Figure 3-14. Typical channel cross section.
Conceptual figure created in Adobe Illustrator 8.0 and stored in:
J:\ShallowInfiltrationRpt\WatershedRpt\NewFigureNames\fig3-14.pdf

Figure 3-17. Figures with spatial distribution of excess infiltration (infiltration into soil horizon minus precipitation) and bedrock infiltration (percolation into bedrock layer, here treated as shallow infiltration, hence out of the reach of evapotranspiration) for storm S8_3995b [storm171L, SAIC station 8, March 9-11, 1995 event]. Precipitation is uniformly distributed over this small watershed, even though we know there are some sheltering effects depending on the wind direction; both orographic and storm size effects are expected to be small because the watershed is small (0.25 km^2). Since KINEROS2 does not include the effect of evapotranspiration (each simulation is started with an average initial condition reflecting a relatively "dry" antecedent condition), the bedrock infiltration is an overestimate where soils are thin. Simulation results are from Woolhiser (sci ntbk #362). Ascii files are created from the simulation results with infiltration values and element identifiers in two columns. These ascii files can be joined to the grid files since they use the same element identifiers. The palettes/color legends are tweaked in ArcView 3.1 to bring out a color variation across the model domain. The distribution of bedrock infiltration is controlled by the locations of thin soil cover, particularly areas where slopes are shallow. The distribution of excess infiltration is controlled by the slope, soil thickness, and number of upstream contributing elements. Below steep slopes with thin soil cover, the runon component is particularly large if there is a thickening of the soil cover at the base of the slope (remember the prominence of saturation induced runoff in the upper watersheds versus Hortonian runoff in Solitario Canyon). Saturation induced runoff is where the infiltrating front reaches the bedrock, then the soil saturates upwards because the bedrock has a lower permeability than the soil cover. Hortonian runoff is where the rainfall intensity is greater than the rate of sorption (sorption rate capability at that pressure head; and near saturation, greater than the saturated permeability). The figure is shown on page 72.
J:\AVData\WatershedGrid\Infiltration\storm171L.txt
J:\AVData\WatershedGrid\storm171.apr and storm171-infilt.apr

Figure 3-17

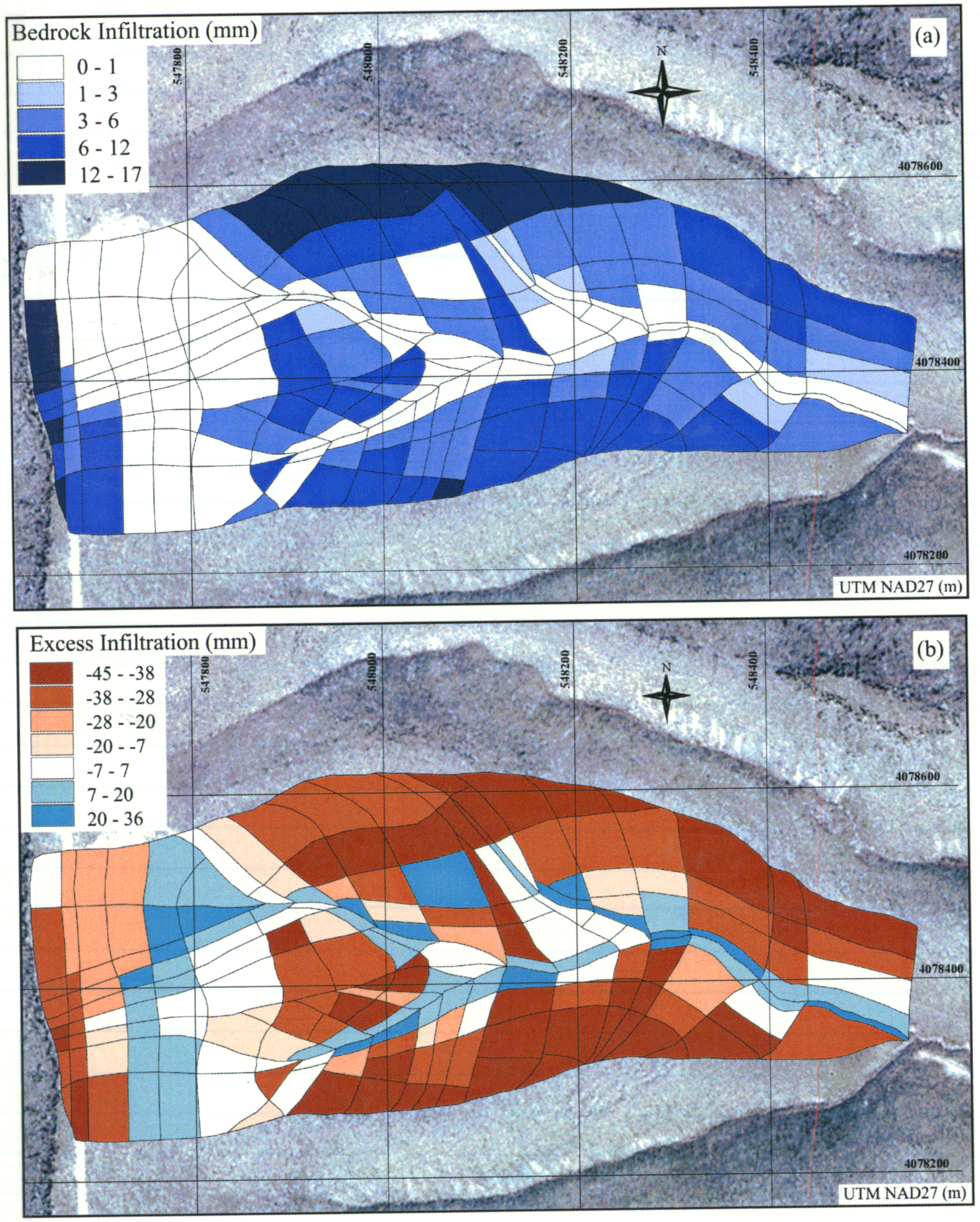

Figure 3-18. Infiltration distributions averaged for all 17 events simulated during the 1987-1995 tipping bucket record. Constructed same way as figure 3-17.

J:\AVData\WatershedGrid\Infiltration\excess1987-95.txt and bedrx-AvgInfilt.txt

J:\AVData\WatershedGrid\infiltration.apr and infilt-bedrock.apr

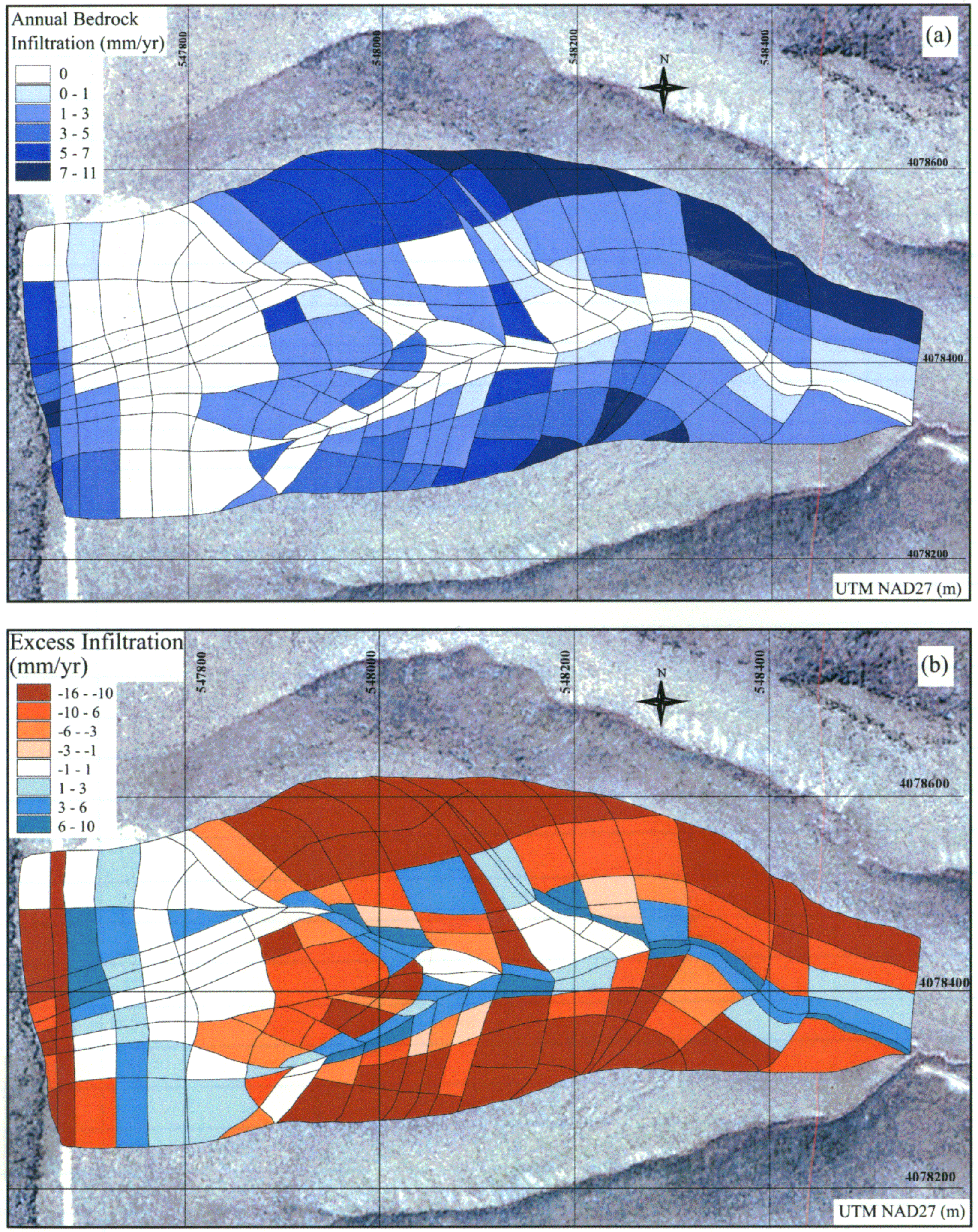

Figure 3-20. Cumulative distributions of Stothoff's 1D regression results and watershed results.
To get the Stothoff regression results, the ITYM preprocessor to TPA4.0 was run with 1000 realizations. The ITYM preprocessor is described in Stothoff's sci ntbk (#163) and my TPA sci ntbk #227. The base case values and distributions are those used for TPA 4.0. ITYM was run on ds9 (SUN Ultra). In the bren directory noted below, the program can be run by executing the c-shell script "it.csh" that calls the executable, which itself uses the hardcoded input file called itym.dat. The results were transferred to

D:\Randy\Woolhiser\SplitWash\Infiltration*

bren: ~rfedors/ITYM_March2000/Present-Day/* [input, output, and executable].

The code (readStuu.f) used to extract only the data from the upper watersheds' portion (all upper watersheds in the repository footprint) of Stothoff's modeling domain is called:

D:\Randy\Woolhiser\SplitWash\Infiltration\readStuu.f

and is included here:

```
program readStu
c This version reads in infiltration values from maidtbl.dat
c (ITYM output).
c Output a file with only upper watershed areas extracted
c for comparison
c with Upper Split Wash

c  Reads Stu's files of 1 column data, reformats the data
c to table array form,
c  and writes to 2 files (so that sigmaPlot can import;
c EXCEL stopped
c  at 256 columns); the 2 files are columns 1-350 and 351-737.

      implicit none
      integer*2  mx, my, i, j, nx, ny, iheaders
      parameter(mx=1000, my=1000)
      integer i1,i2,j1,j2, ict
      real smin, smax, avg, sum, avglog, sumlog
c      integer  ibin(mx)
c      character infile*12, outfile*12, outfile2*12
      character infile*12, outfile*12
      real*4  depth(mx,my), S_infilt(mx,my)

      nx = 300
      ny = 199
      infile = 'maidtbl.txt'
      outfile = 'up-wash.dat'
c      outfile2 = 'swdepth2.dat'
      open(8,file=infile,status='unknown')
      open(9,file=outfile,status='unknown')
c      open(10,file=outfile2,status='unknown')

c File is read row by row starting from the NW corner.
c First account for header lines
      iheaders = 12
      do 10 i = 1, iheaders
          read(8,*)
 10   continue

      do 20 j = 1,ny
       do 20 i = 1,nx
        read(8,*) depth(i,j)
 20   continue

c Extract information for upper watershed area only
c upper watersheds --> 547,640 to 548,100 and 4,076,900 to
c 4,079,730
c UTM NAD27 meters; columns 88-104 and rows 109-204
      i1 = 109
      i2 = 204
      j1 = 88
      j2 = 104

c This section writes out a single column for infiltration
c distribution only
c       do 40 j = j1,j2
c         write(9,'(350f7.3)') ( depth(i,j), i=i1,i2 )
c 40    continue

c Get min, max, and average;
c  zero values set to lowest value (for logs) found in upper
c watersheds
c  (needed for stdev=0 because of zero infiltration).
      ict = 0
      sum = 0.
      sumlog = 0.
      smax = 0.
      smin = 1.e6
      do 50 j = j1,j2
        do 50 i = i1,i2
          smax = max(smax,depth(i,j))
          smin = min(smin,depth(i,j))
          sum = depth(i,j) + sum
          if(depth(i,j).le.1.e-6) depth(i,j) = .00984112
          sumlog = log10(depth(i,j)) + sumlog
          ict = ict + 1
 50   continue
      avg = sum / float(ict)
      avglog = sumlog / float(ict)
      print *, 'min   max    average  average-log'
      print *,  smin, smax, avg, avglog

c Normalize to average and shift mid point zero
c This is done instead of subtracting average so that
c infiltration
c magnitudes are not clouding the comparison with the
watershed results.
      ict = 0
      sumlog = 0.
      smax = 0.
      smin = 1.e6
      do 60 j = j1,j2
        do 60 i = i1,i2
c          S_infilt(i,j) = log10(depth(i,j))
          S_infilt(i,j) = depth(i,j) / avg
          smax = max(smax,S_infilt(i,j))
          smin = min(smin,S_infilt(i,j))
          sumlog = S_infilt(i,j) + sumlog
          ict = ict + 1
 60   continue
      avglog = sumlog / float(ict)
      print *, 'min   max    avglog     '
      print *,  smin, smax, avglog

c Write out data for SigmaPlt histogram
c (columns for infiltration distribution only)
c      write(9,*) 'mm/yr          log'
      write(9,*) 'mm/yr          normalized'
      do 100 j = j1,j2
       do 100 i = i1,i2
         write(9,'(2f12.8)') depth(i,j), S_infilt(i,j)
 100   continue

c This section was used to write to a file for SigmaPlot
c       do 40 j = 1,ny
c         write(9,'(350f7.3)') ( depth(i,j), i=1,350 )
c 40    continue
c
c       do 60 j = 1,ny
c         write(10,'(387f7.3)') ( depth(i,j), i=351,nx )
c 60    continue

      stop
      end
```


The UTM NAD27 coordinates extracted out of Stothoff's domain are :547,640 to 548,100 and 4,076,900 to 4,079,730 in units of meters.

D:\Randy\Woolhiser\SplitWash\Infiltration\maidReal1000.xls
contains the extracted data from .\up-wash.dat file, the latter file was obtained from the readStuu.f code run on the initial file .\maidreal1000.dat. The "maidReal1000" sheet in the EXCEL file sorted the shallow infiltration values and normalized them to the total extracted area of the upper watersheds. The normalized cdf (labeled as figure "1D Regression results" on page 71) could then be plotted on the same graph as the watershed results described below.

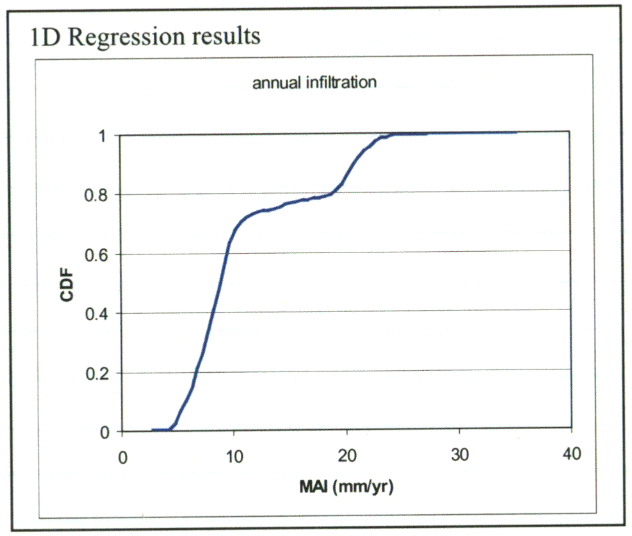

For the 1987-1995 events, a calculated average bedrock infiltration for each element was obtained from Woolhiser (sci ntbk #362). The relative areas of each element were taken from .\Distrib.xls for each element, sorted to match the element ID number, then a cumulative area was calculated and entered into the following spreadsheet. Plots from Pl&cavg.xls file of the pdf and cdf for the watershed average bedrock infiltration are shown below.

D:\Randy\Woolhiser\SplitWash\Infiltration\Pl&cavg.xls

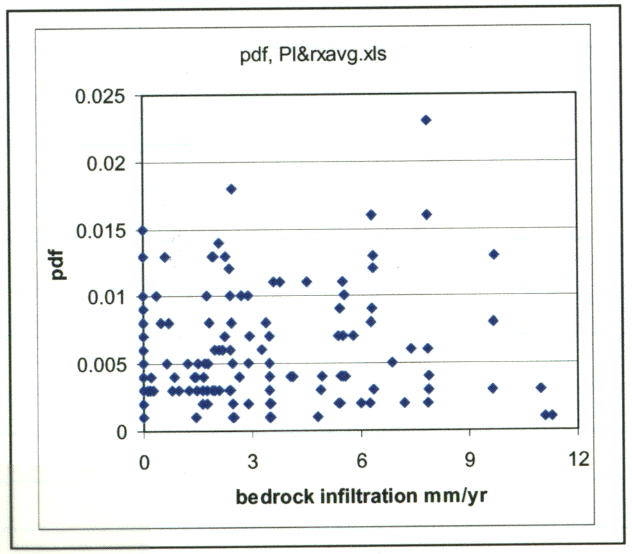

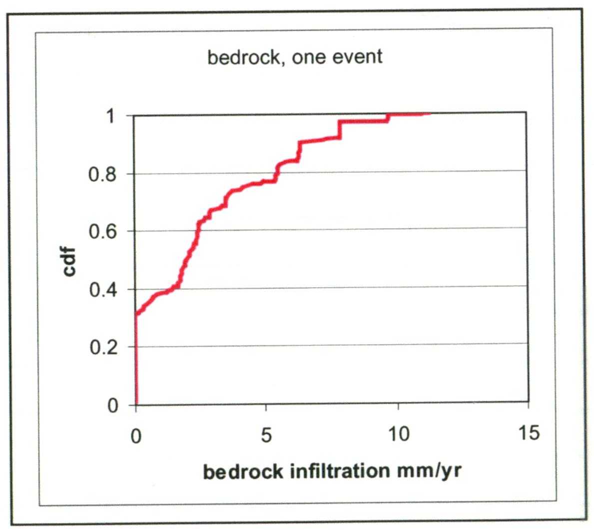

Once plotted, this was now a similarly area-weighted CDF so that the curve could be added to the same plot as the Stothoff cdf described above simply by scaling the bedrock infiltration to [0,1] using the graphical capabilities of Adobe Illustrator 8.0.

Figure 3-21. Probability density function (pdf) of the mean annual shallow infiltration from the 1D regression. The data was developed and extracted as described in figure 3-20 except that instead of a normalized cumulative distribution, a pdf was plotted to illustrate the bimodality of the 1D results.
The EXCEL spreadsheet D:\Randy\Woolhiser\SplitWash\Infiltration\maidReal1000.xls contains the extracted data from .\up-wash.dat file, the latter file was obtained from the readStuu.f code run on the initial file .\maidreal1000.dat. The pdf was obtained by EXCEL sorting and binning (through the use of "if" statements) with a bin size of 0.5 mm/yr. The development of the pdf is contained the file "maidReal1000.xls and is in the sheet labeled "MAI-Real1000".

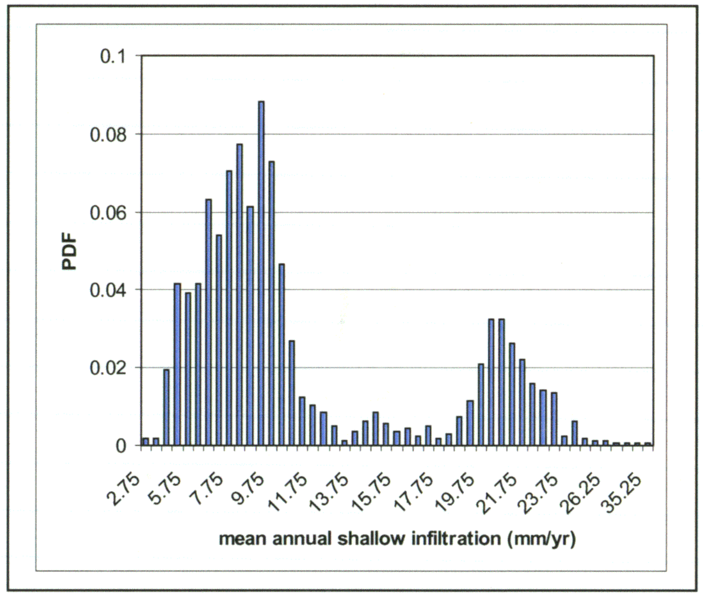

For comparison, the watershed cumulative 1987-1995 results were collected from Woolhiser (sci ntbk #362), normalized to area and to total precipitation amount, sorted, and binned out to plot a pdf. The same bimodality is present though there is a more equal weighting of the two populations for the watershed results. This likely reflects the effect of the runon component that increases infiltration in the lower portions of steep slopes.
D:\ Randy\Woolhiser\SplitWash\Infiltration\Distrib-1.xls sheet labeled "Histograms"

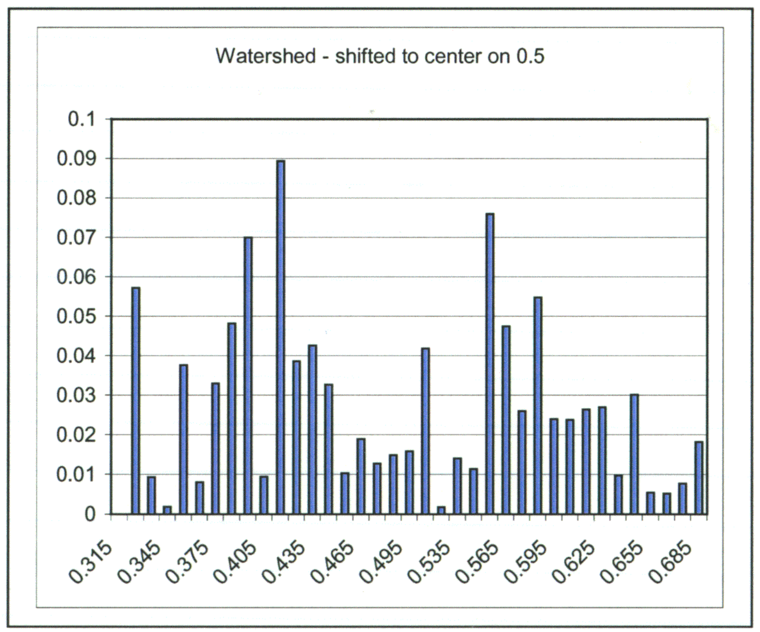

Figure 3-22. Excess infiltration versus soil thickness.
Slope, area, soil thickness for each element are from the grid generation described earlier in this notebook:
D:\Randy\Woolhiser\SplitWash\Grid\DETAIL1a.xls
This information was copied to:
D:\Randy\Woolhiser\SplitWash\Infiltration\Distrib-1.xls in the sheet called "DETAIL1".
Since slope and soil depth of the plane element are related to runon that becomes infiltration (indirectly, since low angle slopes with lots of soil will see the most excess infiltration; however, the runon component is actually related to the upslope element characteristics like number of upslope elements with steep slopes and thin soil cover).

Although slope is also a factor, the simplest relationship was seen in excess infiltration and soil thickness. The disturbed area on top of the crest comprise the outliers in the lower portion of the curve. Conceptually, the most runon should occur in deep sediments below steep slopes covered by thin soils. Here, runon is not only the surface water moving from laterally from upslope locations, but also infers infiltration (think of it as a net runoff/runon for the element).

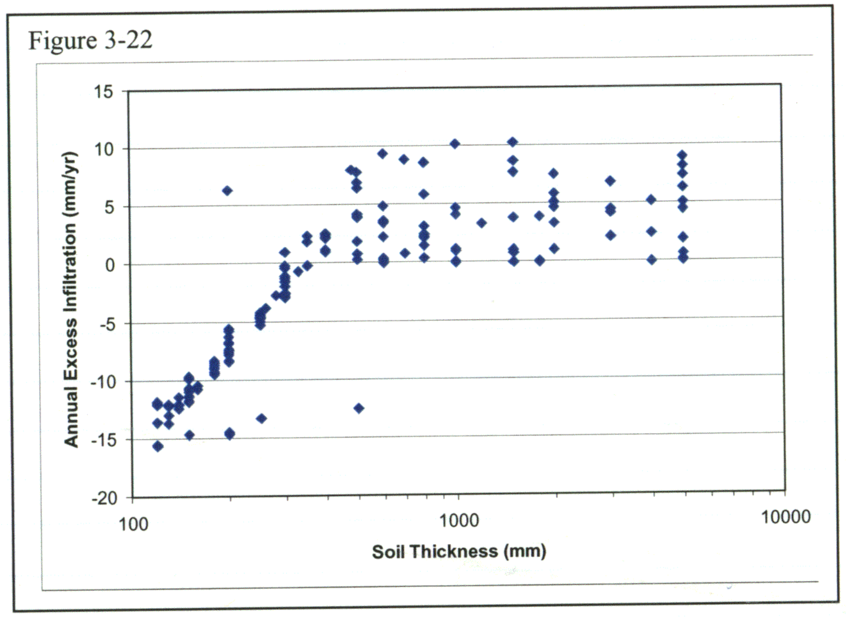

The figure to the right incorporates the slope angle and soil thickness. Note that the hillslope data follows a nice trend for the steep slopes with thin soil (square symbols in negative excess infiltration region). The positive excess infiltration elements show a large scale but do not seem to vary with increasing thickness/slope ratio. Data for "Hillslope only" was extracted by eliminating all elements with saturated permeabilities greater than 0.5 mm/hr (2[nd] layer caprock and alluvium).

Figure created in Distrib-1.xls from data extracted element data from
D:\Randy\Watershed\SplitWash\Grid\DETAIL1.xls

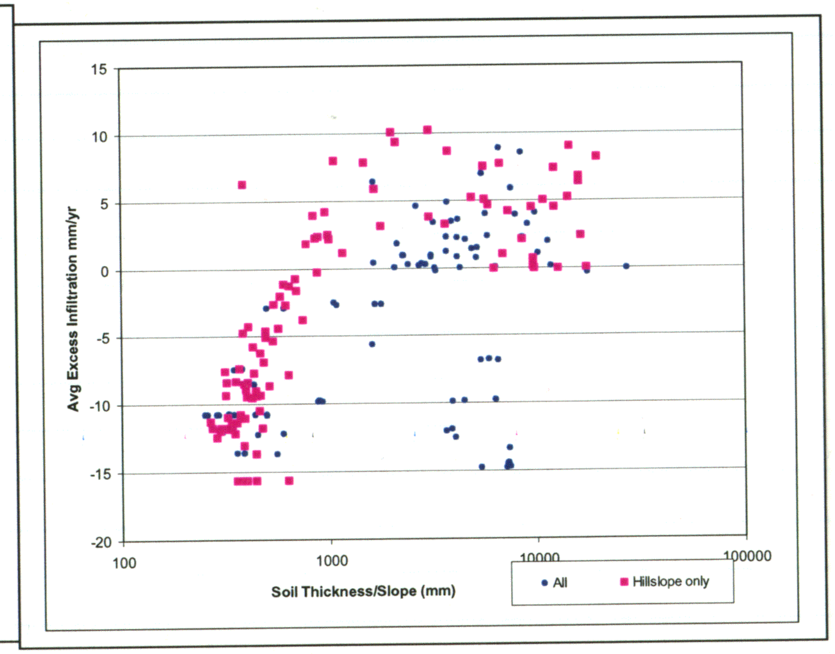

Aggregation of Matrix and Fracture-Fill Properties for Use in 1-Dimensional Infiltration Model 04/25/00

Work done on bubo (WinNT box named bubo, 400 MHz pentium II) and stored in directories:
J:\HydroProperties\Soil-Over-Fracture*
J:\HydroProperties\CompositeProperties*
J:\Hydrus2d*
TOP-018: HYDRUS2D version 2.0 was put under TOP-018 as part of this task
Excel 97 SR-2 will also be used in this work (unmodified, off-the-shelf software)

Objective

Efficient methods for modeling shallow infiltration into a densely welded, fractured, tuff bedrock covered by a thin veneer of uniform soil require innovative modeling approaches. At Yucca Mountain, Nevada, the assumption of predominantly vertical flow and the need for computational efficiency have led to the use of 1D simulations of shallow infiltration. Near the surface, the fractures are either unfilled or filled with caliche or soil material; fracture apertures vary from extremely small to centimeters. An inherent assumption in this simplification is that the matrix and fracture properties of the bedrock can be aggregated into a single equivalent material for the lower (bedrock) portion of the 1D column. Typically, the aggregation is done by assuming the matrix is impermeable and scaling the fracture permeability by the horizontal fracture area. The aggregation of the matrix and fracture properties, however, can easily lead to a modification of the physical problem of flow both across the interface between the layers and through the lower layer. For unfilled fractures, the aggregation may cause a shift from a capillary barrier to a permeability barrier problem, at all flow regimes, with the relationship between the simulated fluxes and the fluxes in the original system being poorly defined. For filled fractures, the aggregation leads to a permeability barrier problem in the 1D model regardless of the properties of the soil or caliche filling the fractures. The aggregation of properties can be viewed as a scaling problem where simulation results from a refined multi-dimensional grid can be used to estimate effective hydrologic properties for the single material representing matrix and fractures in the 1D model. This study uses a 2D numerical approach for modeling a uniform soil layer over a bedrock layer with an explicit fracture to estimate equivalent grid block hydrologic properties for the 1D representation under various flow regimes and proportions of fracture and matrix. Other scaling approaches for aggregating the matrix and fracture properties are evaluated using the finely discretized 2D results for comparison.

Transient simulations are required for two reasons. One, Stothoff's simulations are transient. This work is intended to utilize his existing results, but to better estimate the hydraulic parameters that go into his regressions for the TSPA. Two, steady state flow will produce the same results for flux regardless of the hydraulic properties, unless the capillary barrier effect inhibits flow to the lower cells. If evapotranspiration is included, the transient problem will allow ET to modify the flow out the lower boundary differentially between porous media of different hydraulic properties. Also, the pulses of rain used as influx will have to be varied to make sure that the interplay between influx, initial conditions, and soil properties leads to a consistent conclusion. Various fracture proportions (porosity as used in UZ site-scale model) will be modeled to develop a relation between 2D hydraulic property values and the scaled 1D values. The code to be used for the comparisons is HYDRUS2D.

Comments on Inputs and Discretization of 2D Cases in HYDRUS2D

It is best to start from scratch when using the mesh generator. Conflicts may arise, such as different number of materials between the mesh generator and the main input program, that cause HYDRUS2D to crash or lock out ("out of memory") modules.

Creation of the outer boundary and the objects (polylines) that trace the lithologic contacts and fracture material. In Meshgen2D, use insert lines (*Insert→Numerically*) to create all of the 3 internal lines and the 1 external boundary line.

- The internal lines cannot intersect or coincide with each other or with the outside boundary, so just set them off some small distance (small elements may be created).
- Edit this grid for other fractions of fracture width (based on porosity: 0.5, 0.25, 0.1, 0.01, 0.001, 0.0001) while in *View→Geometry*.

- Add fixed boundary points (insert) while in *View→Boundary Points* mode to help control the density of nodes on the outer boundary
- Also while in *View→Boundary Points* mode, use *Edit→BoundaryPoints→Number of Points* to increase the total number of nodes along an object; use *Edit→BoundaryPoints→Density at Fixed Points* to gradationally space the nodes out along the objects.
- A single point was placed at the "T" intersection of the soil and the fracture.

There was some difficulty in getting the automatic mesh generator to retain the lines the material boundaries. The problem was alleviated by changing the smoothing factor from the default value of 1.3 to a value of 1.6 to 2.0 and by adjusting the number and density of nodes in the boundary segments. The smoothing factor is a ratio of the maximum and minimum dimensions of the triangular elements.

An example of a grid in *View->BoundaryPoint* mode (project in HYDRUS2D is called "sfrac3"):

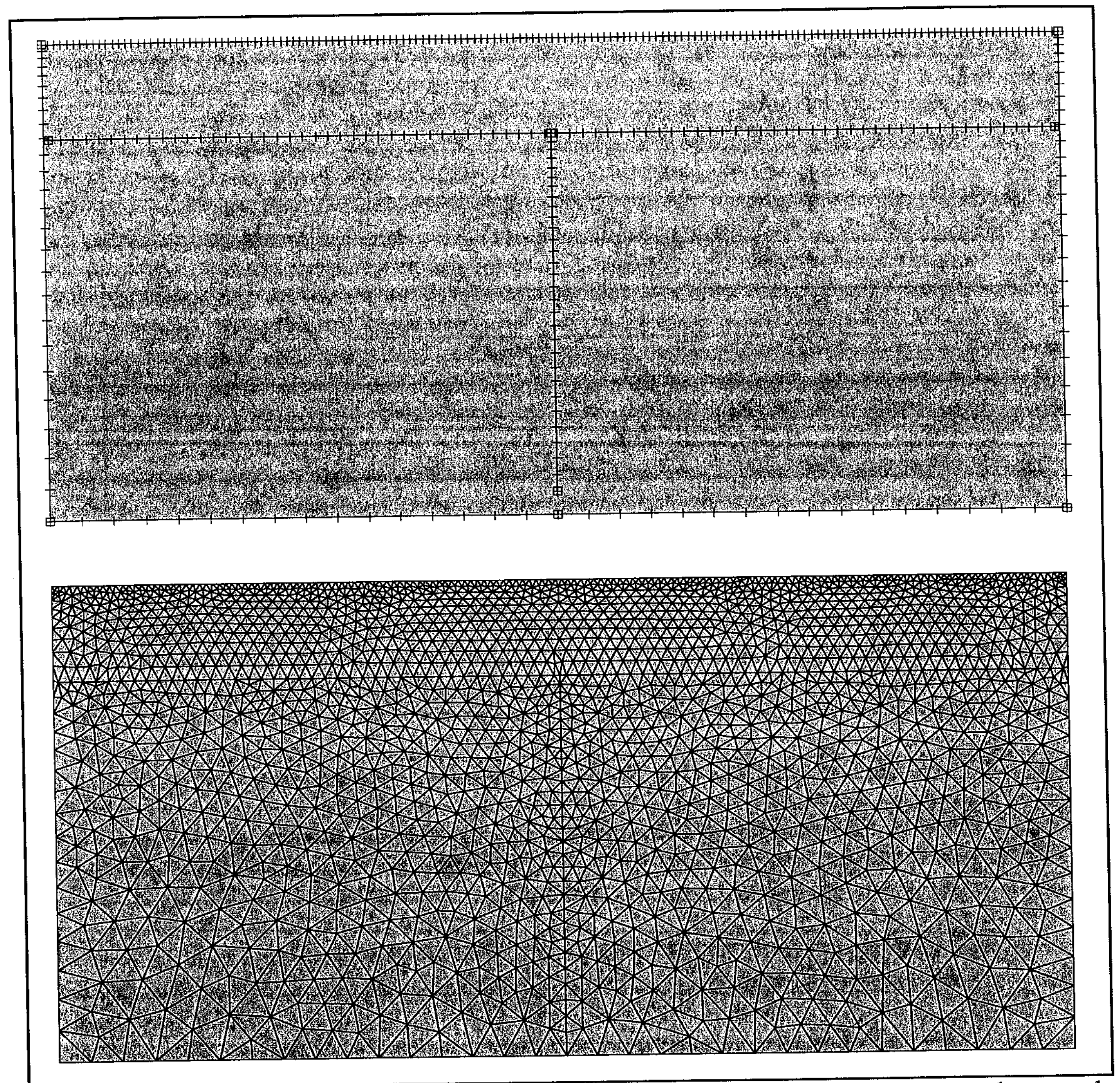

Discussions related to the boundary conditions and sink source terms are included in the next couple pages; but in the end, not all options may be used. Portions of the text are from the HYDRUS2D manual.

Boundary Conditions

The top boundary of the problem will be an atmospheric boundary conditions because evapotranspiration (ET) is expected to be different in the transient case for different porous media hydraulic properties. The transient problem will allow ET to modify the flow. The lower boundary is marked as free drainage. Initial conditions are set to equilibrium from a bottom node set at –1 bar (~10 m of H_2O); the effect of initial conditions on the outflux will need to be checked.

Free Drainage Boundary Condition (Condition Menu)

Free drainage boundary condition. Free drainage is simulated in terms of a unit vertical hydraulic gradient. This situation is often observed in field studies of water flow during drainage/redistribution in the vadose zone [Sisson, 1987; McCord, 1991; see HYDRUS2D documentation for full reference]. McCord [1991] states that the most pertinent application of a free drainage boundary condition is its use as a bottom outflow boundary condition for situations where the water table is situated far below the domain of interest.

Atmospheric Boundary Condition (Condition Menu)

When atmospheric boundary conditions are implemented, time-dependent input data for the precipitation rate, Prec, and the evaporation rate, rSoil, must be specified in the input file ATMOSPH.IN (specified in the major module). The potential fluid flux across the soil surface is determined by rAtm= rSoilPrec. The actual surface flux is calculated internally by the program. Two limiting values of the surface pressure head are needed: hCritS which specifies the maximum allowed pressure head at the soil surface (defaults to 0.0 as noted below), and hCritA which specifies the minimum allowed surface pressure head (defined from equilibrium conditions between soil water and atmospheric vapor). The program automatically switches between Dirichlet and Neumann boundary conditions if one of these two limiting points is reached. The following table summarizes the use of the variables rAtm, hCritS and hCritA during program execution. Width(n) in this table denotes the length of the boundary segment associated with node n.

Definition of the variables Kode(n), Q(n) and h(n) when an atmospheric boundary condition is applied:

Kode(n)	Q(n)	h(n)	Event
-4	Width(n)*rAtm	Unknown	rAtm=rSoilPrec
+4	Unknown	hCritA	Evaporation capacity is exceeded
+4	Unknown	hCritS	Infiltration capacity is exceeded

There is a table of records for the variable boundary conditions. The initial values of Q(n)=0 and h(n)=initial head are assumed therefore the first entry cannot be the time zero record. The variable hCritS is not set in the table. Jirka Simunek (per. comm., 2000) says that the hCritS is not enabled in HYDRUS2D v. 2.0 where it is hardcoded to a value of zero; this implies that runoff occurs immediately. The ascii file ATMOSPH.IN contains this data and is readily edited.

Time (T)		no entry for time = 0
Precipitation (L/T)		
Evaporation (L/T)		
Transpiration (L/T)		
hCritA	$\lvert h_{min} \rvert$	Min allowed pressure head, evaporation capacity exceeded
hCritS	= 0	Max allowed pressure head at surface

Material Types

This figure on the next page illustrates the material boundaries. Materials 1 and 2 are the same when the fractures are soil filled. This figure also shows the fracture porosity at 50%, a rather high value.

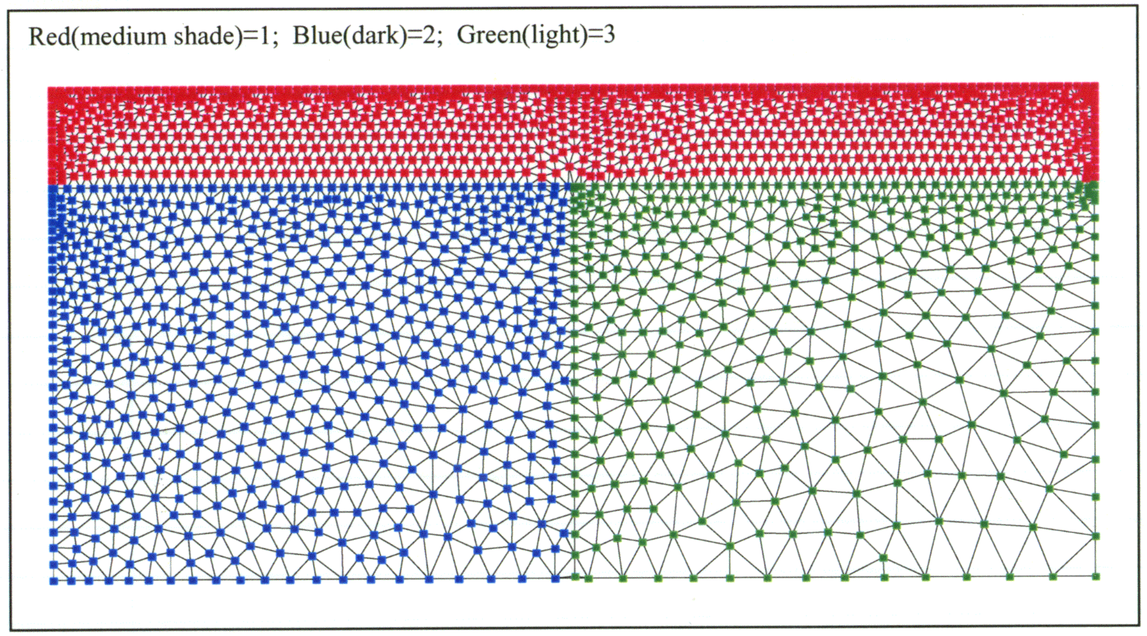

Initial simulation results using the irregular grid in the figure above lead to problematic flux distributions. With an irregular grid, the flux at the surface quickly redistributed leading to a slight focusing of flow. This behavior meant that a uniform top boundary condition was useless purely because of grid effects. Henceforth, a regular grid, refined in special areas, must be used for production runs.

Root Water Spatial Distribution (in Boundary Conditions Editor)

If transpiration is to be used in later simulations (initially it will not be used), then the following description should be useful. The area and depth of root extraction needs to be outlined, and also specify the distribution function. Examples are UNSAT2 problem (page 7-70 of documentation) that uses depths 5 to 40 cm for a potato field; the beta is approximately (from a graph). All of the examples in the HYDRUS2D catalog use the uptake parameter set to 1 and there is always a sharp contrast little gradation in root zone uptake.

Potential root water uptake may be distributed non-uniformly over a root zone of arbitrary shape. The maximum root-water-uptake curve is time independent (scaled to a potential ET rate of unity and assuming no water or salinity stress). However, the root water uptake rate itself may be time dependent. The maximum root-water-uptake curve reflects the distribution in the root zone of roots that are actively involved in water uptake.

The root-water-uptake distribution is specified in two steps. First, the spatial region occupied by the root zone is selected using the mouse; next, the relative intensity of root water uptake, b', is specified in the pop up window. The absolute value of the root uptake intensity is not important since the water uptake distribution is normalized at the beginning of the calculations.

The Root Water Uptake Parameters

The manual gives a schematic of the stress response function as used by Feddes et al. [1978]. Water uptake is assumed to be zero close to saturation (i.e. wetter than some arbitrary "anaerobiosis point" P0). Root water uptake is also zero for pressure heads less than the wilting point (P3). Water uptake is considered optimal between pressure heads Popt and P2, whereas for pressure heads between P2 and P3 (or P0 and Popt) water uptake decreases (or increases) linearly with pressure head.

P0 Value of the pressure head below which roots start to extract water from the soil.
Popt Value of the pressure head below which roots extract water at the maximum possible rate.
P2H Value of the limiting pressure head below which roots cannot longer extract water at the maximum rate (assuming a potential transpiration rate of r2H).
P2L As above, but for a potential transpiration rate of r2L.
P3 Value of the pressure head below which root water uptake ceases (usually taken at the wilting point).
R2H Potential transpiration rate [LT-1] (currently set at 0.5 cm/day).
R2L Potential transpiration rate [LT-1] (currently set at 0.1 cm/day).

The above input parameters permit one to make the variable P2 a function of the potential transpiration rate, Tp (P2 presumably decreases at higher transpiration rates). HYDRUS2 currently implements the same linear interpolation scheme as used in several versions of the SWATRE code (e.g., Wesseling and Brandyk, 1985). The interpolation scheme is defined in the manual.

<u>Hydraulic Properties Used in This Modeling</u>

Base Case Hydraulic Property Summary: Soils [Model Unit 5 covers 46% of the simulation area in Flint, Hevesi, and Flint (1996, draft)]. Bedrock values from Flint

Input for HYDRUS2D

	SOIL	CAPROCK	Tcpmn
θ_r	0.035	.01	0.01
θ_s	0.33	.253	0.082
n	1.78	1.84	1.69
α	5.7 m^{-1}	0.084 m^{-1}	0.012 m^{-1}
K_s	0.58 m/d	0.0033 m/d	5.e-6 m/d
l^*	0.5	0.5	0.5

* van Genuchten suggests that it is typically 0.5

Results from sfrac4 clearly show a non-uniform infiltration that appears to be controlled by the automatic mesh generator locally creating slightly larger elements near the soil surface. Maybe adding internal lines near the ground surface will help control the element sizes, else go to a regular grid.

Since I need the soil and bedrock properties for both this aggregation study and the watershed modeling study in upper Split Wash, I thought I would just collect all sources here.

	ϕ	k m^2	K_{sat} mm/yr	K_{sat} cm/d	α Pa^{-1}	α cm^{-1}	n	S_r
Soil [1] typical	.33	6.85e-13	2.11e+5	5.79e+1	5.6e-4	5.48e-2	1.78	.106
Soil [1] low	.366	5.72e-13	1.77e+5	4.84e+1	5.2e-4	5.09e-2	1.24	.148
Soil [1] high	.281	3.88e-12	1.20e+6	3.28e+2	8.7e-4	8.51e-2	1.62	.007
Soil (Stothoff) [2]	.3	1.e-12	3.09e+5	8.46e+1	5.0e-4	4.90e-2	1.25	0.0
TC (Tcprv) [1]	.048	1.63e-16	5.04e+1	1.38e-2	8.85e-6	8.68e-4	1.249	.2
CUC (Tcprn,rl) [1]	.253	3.89e-15	1.20e+3	3.29e-1	8.27e-6	8.11e-4	1.84	.04
CUL (Tcpul) [1]	.164	1.28e-15	3.94e+2	1.08e-1	1.40e-5	1.38e-3	1.529	.061
TCW (Tcpmn,pll) [1]	.082	5.91e-18	1.83e+0	5.00e-4	1.24e-6	1.22e-4	1.690	.12
tccap [2]	.105	3.2e-16	9.88e+1	2.71e-2	5.00e-6	4.90e-4	1.43	0
tcul [2]	.108	9.1e-19	2.81e-1	7.69e-5	2.94e-6	2.88e-4	1.45	0

	ϕ	k m^2	K_{sat} mm/yr	K_{sat} cm/d	α Pa^{-1}	α cm^{-1}	n	S_r
tschar [2]	.235	1.6e-13	4.94e+4	1.35e+1	3.03e-6	2.97e-4	1.31	0
Tcw11, matrix [3]	.066	5.37e-18	1.66e+0	4.54e-4	1.18e-6	1.16e-4	1.302	.13
Tcw12, matrix [3]	.066	5.37e-18	1.66e+0	4.54e-4	1.32e-6	1.29e-4	1.309	.13
Tcw13, matrix [3]	.140	4.90e-17	1.51e+1	4.14e-3	6.46e-7	6.34e-5	1.745	.33
Tcw11, fracture [3]	2.33e-4	2.29e-11	7.07e+6	1.94e+3	2.95e-4	2.89e-2	1.96	.01
Tcw12, fracture [3]	2.99e-4	1.38e-11	4.26e+6	1.17e+3	2.95e-4	2.89e-2	1.96	.01
Tcw13, fracture [3]	7.05e-5	2.82e-12	8.71e+5	2.38e+2	9.12e-5	8.94e-3	1.96	.01
CCR (rn4) [4]	.062	1.53e-19	4.73e-2	1.30e-5	3.35e-6	3.29e-4	1.254	.20
CUC (rn3,2,1,rl) [4]	.253	3.98e-15	1.23e+3	3.37e-1	8.27e-6	8.11e-4	1.840	.04
CUL (ul) [4]	.164	5.82e-17	1.80e+1	4.92e-3	1.40e-5	1.38e-3	1.529	.06
CW (pmn,pll,pln) [4]	.082	3.88e-19	1.20e-1	3.28e-5	1.15e-6	1.13e-4	1.300	.13
CMW (plnc2,pv3) [4]	.203	8.99e-19	2.78e-1	7.6e-5	2.30e-7	2.26e-5	1.776	.33
CNW (pv2,pv1) [4]	.387	2.66e-14	8.2e+3	2.25e+0	7.52e-5	7.38e-3	1.203	.10
CCR min	avg ϕ	3.4e-20	1.0e-2	2.9e-6				
CCR geom mean	.109	3.3e-18	1.0e+0	2.8e-4				
CCR max		1.2e-15	3.7e+2	1.0e-1				
CUC min	avg ϕ	1.4e-19	4.4e-2	1.2e-5				
CUC geom mean	.233	1.4e-15	4.3e+2	1.2e-1				
CUC max		3.3e-13	1.0e+5	2.8e+1				
CUL min	avg ϕ	6.2e-19	1.9e-1	5.2e-5				
CUL geom mean	.137	2.2e-17	6.8e+0	1.9e-3				
CUL max		5.1e-16	1.6e+2	4.3e-2				
CW min	avg ϕ	7.9e-22	2.4e-4	6.7e-8				
CW geom mean	.093	4.5e-19	1.4e-1	3.8e-5				
CW max		4.3e-13	1.3e+5	3.7e+1				
CMW	no data							
CNW min	avg ϕ	3.7e-20	1.2e-2	3.2e-6				
CNW geom mean	.342	1.5e-15	4.6e+2	1.3e-1				
CNW max		4.3e-13	1.3e+5	3.6e+1				
Tcpmn min [5]	avg ϕ	4.5e-20						
Tcpmn geo mean [5]	.107	1.7e-18						
Tcpmn max [5]		3.5e-17						
Tcpll min [5]	avg ϕ	1.4e-20						
Tcpll geo mean [5]	.088	6.3e-19						
Tcpll max [5]		7.4e-16						
Tcplnh min [5]	avg ϕ	7.9e-22						
Tcplnh geo mean [5]	.070	1.9e-19						
Tcplnh max [5]		2.0e-17						

	ϕ	k m^2	K_{sat} mm/yr	K_{sat} cm/d	α Pa^{-1}	α cm^{-1}	n	S_r
Tcplnc min [5]	avg ϕ	4.1e-20						
Tcplnc geo mean [5]	.110	5.5e-19						
Tcplnc max [5]		4.3e-13						
$H=p/\gamma$ where $\gamma=\rho g$; $n=1(1-m)$; Pa =Pascals=N/m^2, N=kg m/s^2; $S_r=\theta_r/\phi$								
$K_{sat}=k\rho g/\mu$, where $\rho g/\mu$= 97,870.367 $cm^{-1}s^{-1}$; $K_{sat}(mm/yr)=k(m^2)*3.08855e15$								
ρ=0.998g/cm3 g=980.665 cm/s, viscosity=0.01 g/(cm s) (Jury 1991 Soil Physics)								

Footnotes:

1. Flint, Hevesi, and Flint (1996 draft report on infiltration);
Matrix only properties, uses geometric mean of measured hydraulic conductivity from Flint 1998
The values for the soil are from the most widely distributed (46% mapped area) soil unit#5; and unit#4 is at the high range and unit#1 is at the low range;

2. Stothoff WRR submitted paper on infiltration abstractions
Matrix and matrix/fracture hydraulic properties
tccap (caprock; CUC or Tcr2 & Tcr1)
tcul (upper lithophysal; CUL or Tcpul)
tcshar (nonweleded shardy base; CNW or Tcpv2 & Tcpv1)

3. UZ Site-Scale Model
Calibrated matrix and fracture for dual continuum hydraulic properties.
Berkeley didn't pay particular attention of thermo-mechanical units, it appears that they just physically divided the upper half of the Tiva Canyon from the lower half based on depths alone. This is not confirmed,
but at a cross-section through SD-7, Tcw11 included the Tcpmn, Tcpll, and Tcpln (there was no other units above the Tcpmn in SD-7, just colluvium/alluvium).
Tcw11 (upper half, probably all exposed bedrock above repository) | these contain CCR, CUC,
Tcw12 (lower half) | CUL, and CW; ill-defined
Tcw13 (basal vitrophyre)

4. Flint 1998
Matrix properties report, geometric means of permeability, from table summaries.
CCR (vitrophyre of upper cliff of nonlithophysal crystal-rich member: Tcpr inlcuding rn4)
CUC (upper cliff of nonlithophysal crystal-rich member: Tcpr including rn3, rn2, rn1, rl)
CUL (upper lithophysal: Tcpul)
CW (Tcpmn, Tcpll, Tcpln including plnh and plnc; includes clinkstone, hackly, rounded, & columnar)
CMW (lower part of lower nonlithophysal and welded portion of basal vitric: Tcplnc2, Tcpv3v)
CNW (nonwelded portion of basal vitric: Tcpv2, Tcpv1)

5. Flint 1998
Manipulation of matrix properties spreadsheet of Flint; sorted then min, max, and geometric means calculated. Two layer classifications used: (i) Flint's (1997) , and (ii) Day et al. 1998. Day et al. essentially subdivides the CW unit into 3 units. The arithmetic average is used for the porosity while the geometric mean is used for the permeability. Values entered in the table above for data source 5 were calculated in:
J:\HydroProperties\Soil-Over-Fracture\Flint-Tiva.wb3
Sorting and calculation of mean values was done in Quattro because EXCEL 97 is a business spreadsheet package, still trying to catch up on the scientific side of things. Here, QuattroPro (Release 8.0.0.611 in 1997) was used because it was able to calculate geometric means of a series of numbers when there was more than 30 numbers in that series.
Same unit descriptions as descibed in data source 4. above.
A quick look at the measurements of matrix properties by Flint (1997) was done to create average values based on different lithologic classification schemes. I used the spreadsheet from Lorrie Flint that was created for the Flint (1997) report. I sorted

the file to look just at the Tiva Canyon units and calculated arithmetic and geometric means based on the classification schemes used in Flint, Hevesi, and Flint (1996) and the thermal-mechanical scheme used in the Day et al. (1998) central block map (USGS Misc Series Map I-2601).

Ranges and averages of permeabilities of Tiva Canyon units. J:\HydroProperties\Soil-Over-Fractures\flint-Tiva.wb3							
This spreadsheet had to be done in Quattro because Microsoft EXCEL							
could not fathom that one might want to calculate the geometric mean of more than n=30.							
Sorted from Lorrie Flint's spreadsheet of matrix properties.							
arithematic	geometric	median	maximum	minimum			
Ksat	Ksat	Ksat	Ksat	Ksat			
(m/s)	(m/s)	(m/s)	(m/s)	(m/s)	Count	Flint 1997	
1.1E-09	3.2E-11	2.7E-11	1.2E-08	3.3E-13	19	CCR	rn4
1.6E-07	1.4E-08	4.3E-08	3.2E-06	1.4E-12	146	CUC	rn3, rn2, rn1, rl
5.1E-10	2.1E-10	3.2E-10	5.0E-09	6.1E-12	49	CUL	pul
1.8E-08	4.5E-12	3.1E-12	4.2E-06	7.7E-15	654	CW	pmn, pll, plnh, plnc
-	-	-	-	-		CMW	plnc2, pv3v
8.1E-07	1.4E-08	2.5E-07	4.2E-06	3.7E-13	130	CNW	pv2, pv1
						Day et al. 1998	
1.6E-07	1.4E-08	4.3E-08	3.2E-06	1.4E-12	146	rn (3,2,1,rl)	Tcr1, Tcr2
5.1E-10	2.1E-10	3.2E-10	5.0E-09	6.1E-12	49	pul	Tcpul
5.1E-11	1.6E-11	1.9E-11	3.4E-10	4.4E-13	32	pmn	Tcpmn
8.5E-11	6.1E-12	4.6E-12	7.2E-09	1.3E-13	181	pll	Tcpll
4.6E-12	1.8E-12	1.4E-12	2.0E-10	7.7E-15	169	plnh	Tcpln
4.3E-08	5.4E-12	3.4E-12	4.2E-06	4.1E-13	272	plnc	Tcpln
arithematic	geometric	median	maximum	minimum			
k (m2)	k (m2)	k (m2)	k (m2)	k (m2)		Flint 1997	
1.1E-16	3.3E-18	2.7E-18	1.2E-15	3.4E-20		CCR	rn4
1.6E-14	1.4E-15	4.4E-15	3.3E-13	1.4E-19		CUC	rn3, rn2, rn1, rl
5.2E-17	2.2E-17	3.3E-17	5.1E-16	6.2E-19		CUL	pul
1.8E-15	4.5E-19	3.1E-19	4.3E-13	7.9E-22		CW	pmn, pll, plnh, plnc
-	-	-	-	-		CMW	plnc2, pv3v
8.2E-14	1.5E-15	2.6E-14	4.3E-13	3.7E-20		CNW	pv2, pv1
						Day et al. 1998	
1.6E-14	1.4E-15	4.4E-15	3.3E-13	1.4E-19		rn (3,2,1,rl)	Tcr1, Tcr2
5.2E-17	2.2E-17	3.3E-17	5.1E-16	6.2E-19		pul	Tcpul
5.2E-18	1.7E-18	2.0E-18	3.5E-17	4.5E-20		pmn	Tcpmn
8.6E-18	6.3E-19	4.7E-19	7.4E-16	1.4E-20		pll	Tcpll
4.7E-19	1.9E-19	1.4E-19	2.0E-17	7.9E-22		plnh	Tcpln
4.4E-15	5.5E-19	3.4E-19	4.3E-13	4.1E-20		plnc	Tcpln
arithematic	geometric	median	maximum	minimum			
Ksat mm/yr	Ksat mm/yr	Ksat mm/yr	Ksat mm/yr	Ksat mm/yr		Flint 1997	
3.5E+01	1.0E+00	8.5E-01	3.7E+02	1.0E-02		CCR	rn4
4.9E+03	4.3E+02	1.4E+03	1.0E+05	4.4E-02		CUC	rn3, rn2, rn1, rl
1.6E+01	6.8E+00	1.0E+01	1.6E+02	1.9E-01		CUL	pul
5.7E+02	1.4E-01	9.6E-02	1.3E+05	2.4E-04		CW	pmn, pll, plnh, plnc
-	-	-	-	-		CMW	plnc2, pv3v
2.5E+04	4.6E+02	7.9E+03	1.3E+05	1.2E-02		CNW	pv2, pv1
						Day et al. 1998	
4.9E+03	4.3E+02	1.4E+03	1.0E+05	4.4E-02		rn (3,2,1,rl)	Tcr1, Tcr2
1.6E+01	6.8E+00	1.0E+01	1.6E+02	1.9E-01		pul	Tcpul
1.6E+00	5.2E-01	6.1E-01	1.1E+01	1.4E-02		pmn	Tcpmn
2.7E+00	1.9E-01	1.5E-01	2.3E+02	4.2E-03		pll	Tcpll
1.5E-01	5.8E-02	4.5E-02	6.2E+00	2.4E-04		plnh	Tcpln
1.4E+03	1.7E-01	1.1E-01	1.3E+05	1.3E-02		plnc	Tcpln
arithematic	geometric	median	maximum	minimum			
Ksat cm/d	Ksat cm/d	Ksat cm/d	Ksat cm/d	Ksat cm/d		Flint 1997	
9.6E-03	2.8E-04	2.3E-04	1.0E-01	2.9E-06		CCR	rn4
1.3E+00	1.2E-01	3.7E-01	2.8E+01	1.2E-05		CUC	rn3, rn2, rn1, rl
4.4E-03	1.9E-03	2.7E-03	4.3E-02	5.2E-05		CUL	pul
1.6E-01	3.8E-05	2.6E-05	3.7E+01	6.7E-08		CW	pmn, pll, plnh, plnc
-	-	-	-	-		CMW	plnc2, pv3v
7.0E+00	1.3E-01	2.2E+00	3.6E+01	3.2E-06		CNW	pv2, pv1
						Day et al. 1998	
1.3E+00	1.2E-01	3.7E-01	2.8E+01	1.2E-05		rn (3,2,1,rl)	Tcr1, Tcr2
4.4E-03	1.9E-03	2.7E-03	4.3E-02	5.2E-05		pul	Tcpul
4.4E-04	1.4E-04	1.7E-04	2.9E-03	3.8E-06		pmn	Tcpmn
7.3E-04	5.3E-05	4.0E-05	6.2E-02	1.1E-06		pll	Tcpll
4.0E-05	1.6E-05	1.2E-05	1.7E-03	6.7E-08		plnh	Tcpln
3.7E-01	4.6E-05	2.9E-05	3.7E+01	3.5E-06		plnc	Tcpln

This table was created from reported values and includes conversions to other length and time units.

J:\HydroProperties\Soil-Over-Fractures\flint-Tiva.wb3		e.g. (1/bar) * 10e-5 = 1/Pa
Conversions of published data	100000	Pa/bar
	0.0101972	cm/Pa
h=p/(rho*g) Selker et al. (1999) p. 30	1019.72	cm/bar
Vadose Zone Processes		
	3.088553893E+17	->m2*coef=mm/yr
K=k*rho*g/u	31557600000	->m/s*coef=mm/yr
bulk density = rho =.998 g/cm3 at 20deg C	8640000	->m/s*coef=cm/d
gravity accel = g= 980.665 cm/s2		
viscosity = u = .01 g/cm/s		

Flint 1997	Ksat	alpha		k	Ksat	Ksat	alpha	alpha
	m/s	1/bars		m2	mm/yr	cm/d	1/Pa	1/cm
CCR	1.50E-12	0.335		1.53E-19	4.73E-02	1.30E-05	3.35E-06	3.29E-04
CUC	3.90E-08	0.827		3.98E-15	1.23E+03	3.37E-01	8.27E-06	8.11E-04
CUL	5.70E-10	1.404		5.82E-17	1.80E+01	4.92E-03	1.404E-05	1.38E-03
CW	3.80E-12	0.115		3.88E-19	1.20E-01	3.28E-05	1.15E-06	1.13E-04
CMW	8.80E-12	0.023		8.99E-19	2.78E-01	7.60E-05	2.3E-07	2.26E-05
CNW	2.60E-07	7.522		2.66E-14	8.20E+03	2.25E+00	7.522E-05	7.38E-03
Berkeley	k	alpha			Ksat	Ksat		alpha
	m2	1/Pa		m2	mm/yr	cm/d	1/Pa	1/cm
tcw11 m	5.37E-18	1.18E-06		5.37E-18	1.66E+00	4.54E-04	1.18E-06	1.16E-04
tcw12 m	5.37E-18	1.32E-06		5.37E-18	1.66E+00	4.54E-04	1.32E-06	1.29E-04
tcw13 m	4.90E-17	6.46E-07		4.90E-17	1.51E+01	4.14E-03	6.46E-07	6.34E-05
tcw11 frac	2.29E-11	2.95E-04		2.29E-11	7.07E+06	1.94E+03	2.95E-04	2.89E-02
tcw12 frac	1.38E-11	2.95E-04		1.38E-11	4.26E+06	1.17E+03	2.95E-04	2.89E-02
tcw13 frac	2.82E-12	9.12E-05		2.82E-12	8.71E+05	2.38E+02	9.12E-05	8.94E-03
Flint, Hevesi, Flint								
	Ksat	alpha		k	Ksat	Ksat	alpha	alpha
	mm/d	1/bar		m2	mm/yr	cm/d	1/Pa	1/cm
rv	0.138	0.885		1.63E-16	5.04E+01	1.38E-02	8.85E-06	8.68E-04
rn	3.291	0.827		3.89E-15	1.20E+03	3.29E-01	8.27E-06	8.11E-04
pul	1.079	1.404		1.28E-15	3.94E+02	1.08E-01	1.40E-05	1.38E-03
pmn, pll	0.005	0.124		5.91E-18	1.83E+00	5.00E-04	1.24E-06	1.22E-04
Soils, Flint								
	Ksat	alpha		k	Ksat	Ksat	alpha	alpha
	m/s	1/Pa		m2	mm/yr	cm/d	1/Pa	1/cm
soil#5	6.70E-06	0.00056		6.85E-13	2.11E+05	5.79E+01	5.60E-04	5.49E-02
soil#4,high	3.80E-05	0.00087		3.88E-12	1.20E+06	3.28E+02	8.70E-04	8.53E-02
soil#1,low	5.60E-06	0.00052		5.72E-13	1.77E+05	4.84E+01	5.20E-04	5.10E-02
	Ksat	1/alpha		k	Ksat	Ksat	alpha	alpha
Stothoff	mm/yr	kPa		m2	mm/yr	cm/d	1/Pa	1/cm
soil#1,low	3.10E+05	2		1.00E-12	3.10E+05	8.49E+01	5.00E-04	4.90E-02
	k m2	kPa						
tccap	3.20E-16	200		3.20E-16	9.88E+01	2.71E-02	5.00E-06	4.90E-04
tcpul	9.10E-19	340		9.10E-19	2.81E-01	7.69E-05	2.94E-06	2.88E-04
tcshar	1.60E-13	330		1.60E-13	4.94E+04	1.35E+01	3.03E-06	2.97E-04

When aggregating the filled-fracture and the bedrock from a 2D to 1D parameter value, the physics of the problem can readily be changed. Whereas the 2D problem is one of funneling the flow along the soil/bedrock contact to filled-fractures and downward, the aggregation can create a permeability barrier in the 1D problem that could entirely modify the movement of a pulse of water down the column.

For unfilled fractures, the aggregation may cause a shift from a capillary barrier to a permeability barrier problem at all flow regimes. For filled fractures, the aggregation leads to a permeability barrier problem in the 1D model regardless of the properties of the soil or caliche filling the fractures. The difficulty in aggregating the properties for the unfilled fracture (caused by the shift in physical processes depending on the flow regime) make it extremely unreliable. It will not be treated in this work because of the following logic argument. All fractures are expected to be filled, whether there is a soil layer or it is bare bedrock, down to apertures in the 25 µm range (these would be too small for soil particles to move into the fracture). Besides, the smallest fracture apertures can be assumed to be reflected in core scale measurements of matrix properties.

Hence, I only need to treat filled fractures. I will only use soil-filled fractures here even though caliche filled fractures are abundant under the assumption that the same aggregation methodology should work for both.

J:\HydroProperties\Soil-Over-Fracture\unsat-properties.xls

The van Genuchten parameters for the soil, caprock and middle nonlithophysal unit are plotted below using the equation for water retention (van Genuchten, 1980; Sci. Soc. Am. J. 44:892-898):

$$S_e = [1 + |ay|^n]^{-m} \quad \text{where} \quad S_e = (\theta - \theta_r)/(\theta_s - \theta_r)$$

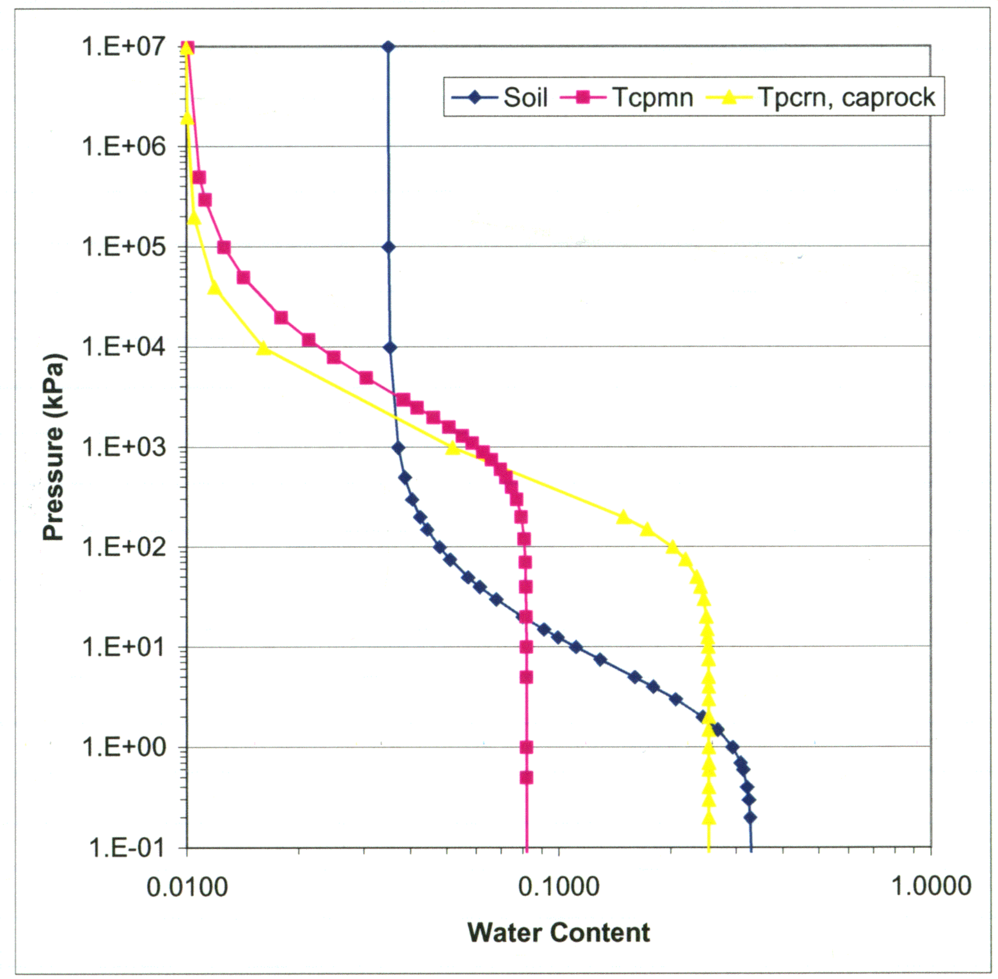

For the plots on this page, the form of the van Genuchten effective permeability constitutive relation used is:

$$K_{eff} = K_{sat}\{S^{1/2}[1-(1-S^{1/m})]^m\}^2 \quad \text{or} \quad K_{eff} = K_{sat}\frac{\{1-|ah|^{n-1}[1+|ah|^n]^{-m}\}^2}{[1+|ah|^n]^{m/2}} \quad \text{where } m = 1-\frac{1}{n}$$

Note that as the fracture porosity scaling of the Ksat becomes more extreme, the problem is coming closer to being strictly a permeability barrier (not quite) instead of transition to higher flow rates possible in the bedrock at the low pressures. Also, these changes are sweeping through the modeling area of interest in transient problems

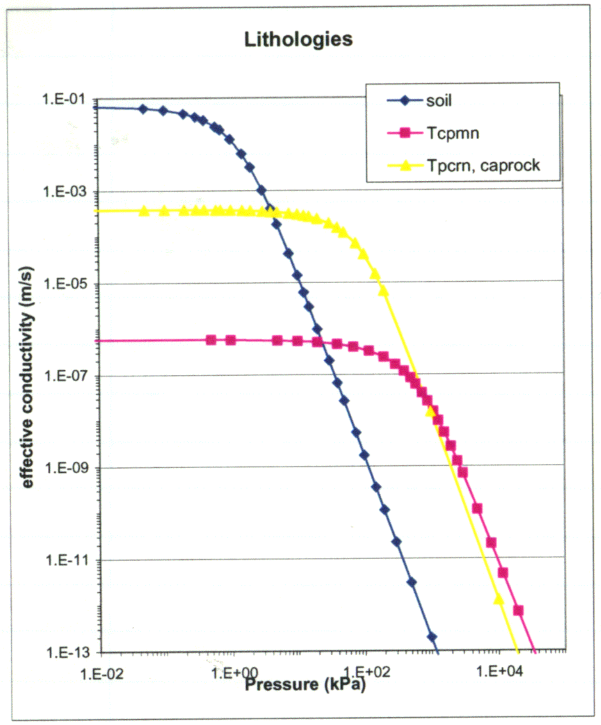

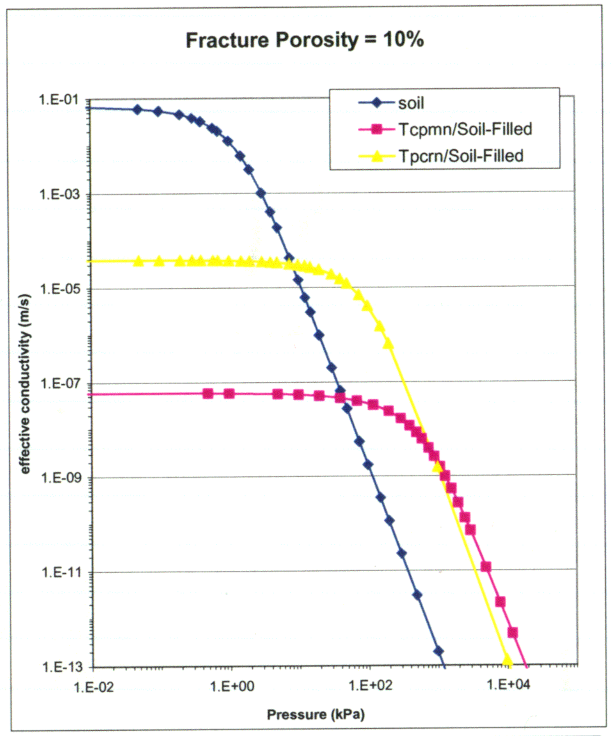

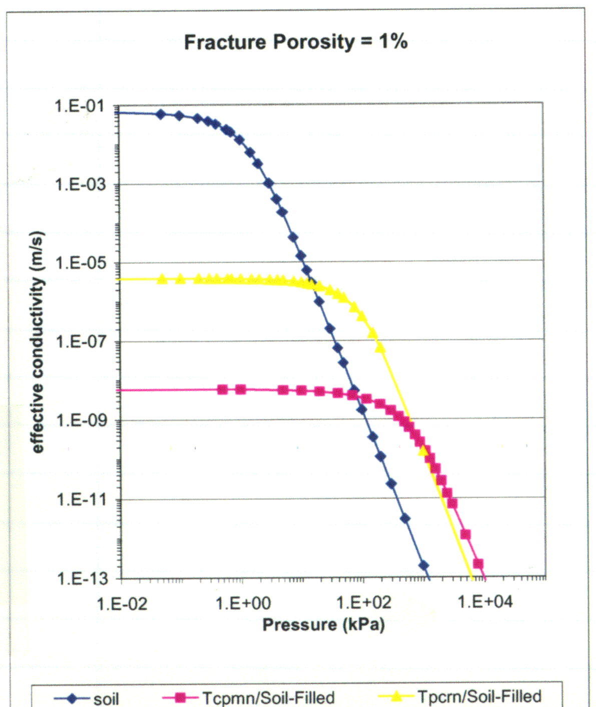

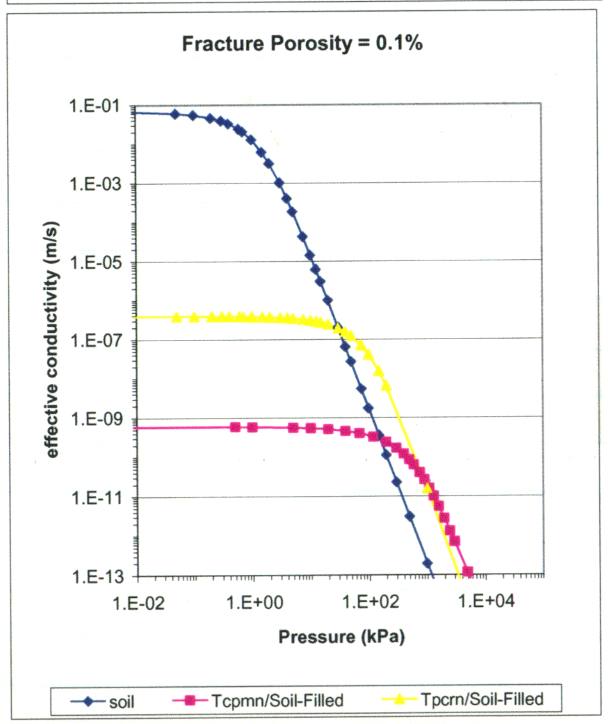

Production Run Setup: 1% and 10% Fracture Porosity Cases

Since there was a problem with using the irregular (automatically generated) grid, time to switch to using a regular grid, though uneven spacing (to reduce number of cells). This should avoid the problem of a uniform top boundary flux becoming non-uniform as it passes through the first set of elements in the grid.

Free drainage for bottom, no flow for the sides, and variable specified flux for top boundary conditions.

The test objective will be to check the peak value, shape, and temporal location of a pulse of water passing out the bottom of the domain. The 2D result will be taken as truth and the 1D results using different methods of aggregating hydraulic properties will be the test. After initial conditions are established at some low steady state flux, precipitation will be applied as a variable flux boundary condition at the top: 12 mm/yr infiltration, which translates to 3.285e-3 cm/d. I will apply 2 cm precipitation event and I will do it as 1 rain event over a 1.2 hour period (0.05 days). The 2 cm event translates to a 40cm/d rate over 1.2 hours (0.5 days).

Set initial conditions to –200 cm at bottom, then static equilibrium from there upward. Then simulate with steady precipitation rate of 12 mm until approximate steady state conditions occur throughout the profile. This time to steady state varies with hydraulic properties. Used restart option with initial conditions from previous simulation results. Once steady state conditions were determined, the initial conditions were imported into the case with the pulse of water at the top boundary.

period	Time (d)	Precip cm/d	Evap.	Transpirat.	hCritA	rGWL	GWL
1	0.001	0.003285	0	0	10000	0	0
2	359.999	0.003285	0	0	10000	0	0
3	360	40	0	0	10000	0	0
4	360.049	40	0	0	10000	0	0
5	360.05	0	0	0	10000	0	0
6	720	0	0	0	10000	0	0

The options were set as follows: water flow only, no root zone uptake, units of cm and days, final time 720 days, initial time step=0.001 days, minimum time step=1e-5 days, max time step 1 day, number of time variable boundary conditions, max iterations=50, water content tolerance=0.0002, pressure head tolerance=0.01, van Genuchten relationship used without hysteresis. Some of these parameters were changed when oscillations were noted in the results (see later entry). The atmospheric boundary condition is used so that I can have a variable precipitation rate, but I set the evaporation and transpiration to zero to keep the problem simple and not confuse the results

Variable cell spacing in vertical direction: the list in the GUI is bottom to top ordering. Also, note that GUI wants the coordinates, not the cell spacing; therefore add one extra coordinate to previous submenu when it requests the number of vertical columns and the number of horizontal columns (the number of columns is 1 minus the entry). The 2D region is 100cm by 50 cm with 76 vertical and 40 horizontal columns whereas the 1D region is 1cm by 50 cm with 2 columns and 40 rows. The same vertical discretization is used for both the 1D and 2D grids. All grids are refined in the vertical directions (Δz) from 0.1cm near the ground surface, bedrock contact and bottom of domain to a maximum cell size of 3 cm. The 1% grid is horizontally refined to 0.1cm in and near the fracture and has a maximum horizontal cell size of 3cm. The 10% grid is horizontally refined to 1cm in and near the fracture and has a maximum horizontal cell size of 2cm. The grids are shown in the next figure with the color representing material types (bedrock or soil or soil-filled fracture).

Three regions (the soil top layer, the bedrock block, and the soil-filled fracture) are labeled with 3 material-type areas as shown in the figure indifferent colors.

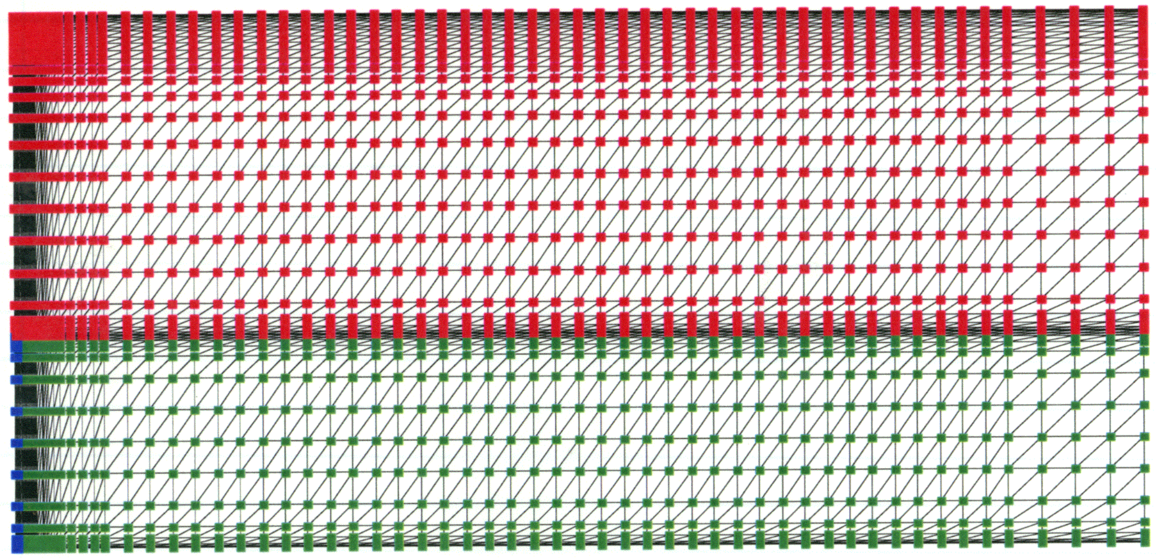

Material: 1=soil (red, upper), 2=soil in fracture (blue, lower left), and 3=bedrock (green, lower right)
Example of 1% fracture porosity case

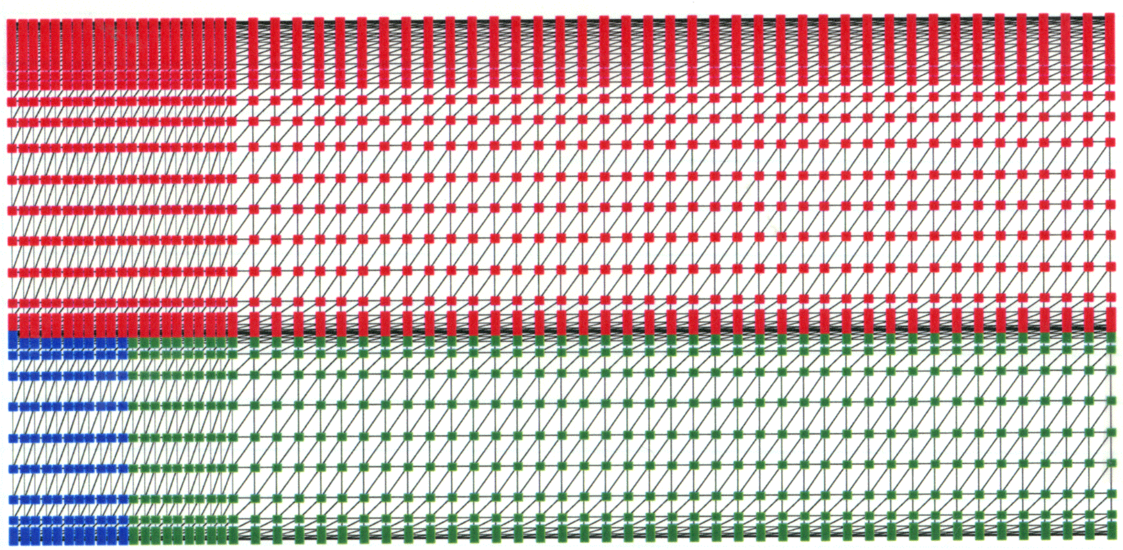

Example of 10% fracture porosity case

Averaging Method

Estimating 1D equivalent hydraulic properties from 2D simulations can be done using the brute force method or using analytical expressions published in the literature for special cases. The brute force method used here is the most robust, and is specifically needed here because of the large difference in properties between the matrix and fracture continua. Published methods of upscaling, for example, are restricted to less that a couple orders of magnitude difference between saturated permeabilities of adjacent cells. In addition, there is no clear guidelines for which UZ properties to scale. The simplest, and thus most defensible is to only scale the permeability and porosity.

Below is a schematic sketch of upscaling the real system to the idealized 1D domain. The exclusion of the effect of the third dimension on this process probably has much less effect than the difference between the 1D and 2D cases. This is because the principle direction of flow is 1D along the bedrock surface, which is an assumption. The use of fracture density would account for flow that could be intercepted by fractures of differing orientations, or, one could just use fracture of a particular orientation relative to a hillslope aspect.

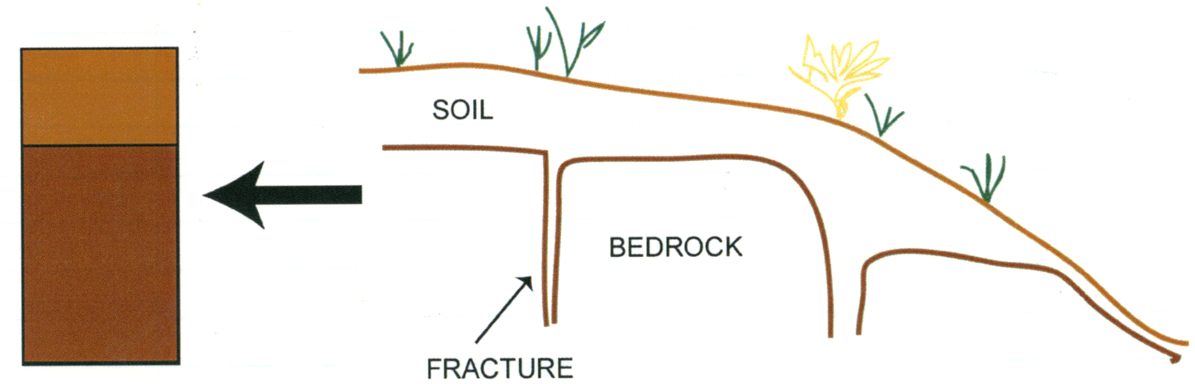

Methods for tweaking the unsaturated parameters tested here will delve into using: (i) geometric, arithmetic, or harmonic means, (ii) weighting based on fracture porosity, and (iii) which UZ parameters to scale, e.g. permeability, van Genuchten α and exponent m, and porosity (k, α, m, ϕ).

Methods:

1. Scale the soil properties of k and ϕ by the fracture porosity. This is called simple scaling and is used by Stothoff. Note that the matrix is assumed to not participate at all. Also note that Stothoff uses the highest shallow infiltration values for the cases of (i) no fracture, (ii) filled fracture, and (iii) fractures with no fill. Hence, Stothoff covers the bases so to speak (this work does not contradict his, it really is an alternative approach that he may be able to use).
2. Weight the soil and bedrock matrix UZ properties; just k and ϕ, or also weight α and m; also could use different weighting schemes for different parameters.

Flint et al. (1996) use a weighting scheme of the soil and bedrock matrix permeabilities. This was not clear from their document so the following page recalculates their values in an attempt to figure out their methodology.

Making sense out of data in Table 2 of Flint et al. 1996							
J:\HydroProperties\CompositeProperties\flint-table2.xls							
			2.5	25	250		
	Ksat, matrix	F/m	m2/m2	m2/m2	m2/m2		
	mm/day		Labeled in Table 2 of Flint et al. as percent				
TCW, undiff.	0.005	10.5	2.60E-05	2.60E-04	2.60E-03		
TC, caprock	0.138	17	4.30E-05	4.30E-04	4.30E-03		
CUC, upper cliff	3.291	9.2	2.30E-05	2.30E-04	2.30E-03		
CUL, upper lith.	1.079	7.8	2.00E-05	2.00E-04	2.00E-03		
Flint et al. (1996) Table 2 entries for composited values							
TCW, undiff.	0.005	0.0015	4.126	1955.63	0.006	0.016	0.118
TC, caprock	0.138	0.156	6.811	3166.39	0.14	0.157	0.322
CUC, upper cliff	3.291	3.3	6.902	1716.79	3.292	3.301	3.39
CUL, upper lith.	1.079	1.087	4.141	1453.83	1.08	1.088	1.163
		soil Ksat	43.2	Flint et al. (1996) page 36, composite			
			0.005	0.005	0.006	TCW, undiff.	
1. Assume Table 2 is a percent			0.138	0.138	0.140	TC, caprock	
wt'd matrix K			3.291	3.291	3.292	CUC, upper cliff	
			1.079	1.079	1.080	CUL, upper lith.	
			0.005	0.005	0.006	TCW, undiff.	
2. Assume Table 2 is a percent			0.138	0.138	0.140	TC, caprock	
no wt'd matrix K			3.291	3.291	3.292	CUC, upper cliff	
			1.079	1.079	1.080	CUL, upper lith.	
			0.006	0.016	**0.117**	TCW, undiff.	
3. Assume Table 2 is a fraction			0.140	0.157	**0.323**	TC, caprock	
weighted matrix K			3.292	**3.300**	**3.383**	CUC, upper cliff	
			1.080	**1.087**	1.163	CUL, upper lith.	
			0.016	0.112	1.075	TCW, undiff.	
4. Assume Table 2 is a fraction			0.149	0.247	1.231	TC, caprock	
and fracture frequency			3.302	3.399	4.371	CUC, upper cliff	
			1.090	1.190	2.187	CUL, upper lith.	
			0.006	0.016	**0.117**	TCW, undiff.	
5. Assume Table 2 is a fraction			0.140	0.157	**0.324**	TC, caprock	
do not weight matrix K			3.292	3.301	3.390	CUC, upper cliff	
			1.080	1.088	**1.165**	CUL, upper lith.	
Items in bold are slightly different from Flint et al (1996) Table 2, otherwise methods 3 & 5 match Flint.							
Conclusion is that columns in Table 2 of Flint et al. (1996) are improperly labeled as percent.							
It is not clear whether the matrix K is weighted though the fracture fill is definitely weighted.							

To facilitate the entering of hydraulic property values, a chart was created in the spreadsheet page called "average" in J:\HydroProperties\simulations.xls

J:\Soil-Over-Fracture\simulations.xls							
Tpcrn Ksat	0.33						
Tcpmn Ksat	5.E-04			10%	(1-f)%		
soil Ksat =	58		Fracture proportion =	0.1	0.9		
		Kavg, wt'd	Kgeom	Kg, wt'd	Khar, wt'd	Stothoff	Flint
	Tpcrn	6.097	4.375	0.553	0.366	5.8	6.130
	Tcpmn	5.800	0.170	1.60E-03	5.56E-04	5.8	5.801
				1%	(1-f)%		
			Fracture proportion =	0.01	0.99		
		Kavg, wt'd	Kgeom	Kg, wt'd	Khar, wt'd	Stothoff	Flint
	Tpcrn	0.907	4.375	0.348	0.333	0.58	0.910
	Tcpmn	0.580	0.170	5.62E-04	5.05E-04	0.58	0.581
				0.1%	(1-f)%		
			Fracture proportion =	0.001	0.999		
		Kavg, wt'd	Kgeom	Kg, wt'd	Khar, wt'd	Stothoff	Flint
	Tpcrn	0.388	4.375	0.332	0.330	0.058	0.388
	Tcpmn	0.058	0.170	5.06E-04	5.01E-04	0.058	0.059
		10%	1%	0.1%			
	porosity	mixture	mixture	mixture	Average		
Tpcrn	0.253	0.2607	0.25377	0.253077	0.2915		
Tcpmn	0.082	0.1068	0.08448	0.082248	0.206		
soil	0.33						
residual water content		0.0125	0.01025	0.010025			
Tcpmn & Tpcrn							
		10%	1%	0.1%			
	alpha	mixture	mixture	mixture	Average		
Tpcrn	8.E-04	6.22E-03	1.34E-03	9.E-04	0.0279		
Tcpmn	1.2E-04	5.61E-03	6.69E-04	1.7E-04	0.02756		
soil	0.055						
		10%	1%	0.1%			
	n	mixture	mixture	mixture	Average		
Tpcrn	1.84	1.834	1.8394	1.83994	1.81		
Tcpmn	1.69	1.699	1.6909	1.69009	1.735		
soil	1.78						
				Soil	Tpcrn	Tcpmn	
			porosity	0.33	0.253	0.082	
			residual water content	0.035	0.01	0.01	
			van Genuchten alpha (1/cm)	0.055	8.E-04	1.2E-04	
			van Genuchten "n"	1.78	1.84	1.69	
			Ksat (cm/d)	58	0.33	5.E-04	

The production runs are located in: J:\Hydrus2d\One* 6/29/00
J:\Hydrus2d\Ten*
and are named (where the question marks refer to individual simulations denoted by letters of the alphabet; e.g., sf1d-3a is the simulation to determine the steady state initial conditions for sf1d-3aa):

sf1d-3? and sf2d-3??
sf1d-4? and sf2d-4??
sf1d-5? and sf2d-5??
sf1d-7? and sf2d-7??

The 2D simulations are named in a similar manner except that one less letter is used at the end of the file name:

sf1d-3 and sf2d-3a
sf1d-4 and sf2d-4a
sf1d-5 and sf2d-5a
sf1d-7 and sf2d-7a

The simulations with hydrologic properties are listed in a table on the following page and are stored in spreadsheet:
J:\HydroProperties\Soil-Over-Fracture\runs-summary.xls

The results are imported into the spreadsheet J:\HydroProperties\Soil-Over-Fracture\simulations.xls by reading in the v_Mean.out output created by HYDRUS2D; the last column is flux out the bottom over time. The plots will be analyzed visually to determine if the 1D pulse comes close to matching the 2D pulse. To match the 2D results (100 cm horizontal domain), the 1D results have to multiplied by 100 since the 1D grid was 1 cm wide.

For the Tcpmn 2D simulations, the bedrock matrix did not dampen the pulse going through the fracture, hence smaller maximum Δt=-0.05 d, minimum Δt =1e-6 d, and tolerances for water content (.0001 instead of the default of 0.0002) and pressure head (0.001cm instead of 0.01cm) were used. I believe the smaller maximum Δt made the bigger difference. These changes were also made for 1D simulations that oscillated; these were primarily the scaled Ks and porosity simulations (small porosity of lower layer lead to the pulse shooting the gap, so to speak). Based on screen output, the time steps get down to **less than** 1.e-4 d. Apparently the max Δt reduction eases the burden when the pulse suddenly appears at day 360 of the simulation.

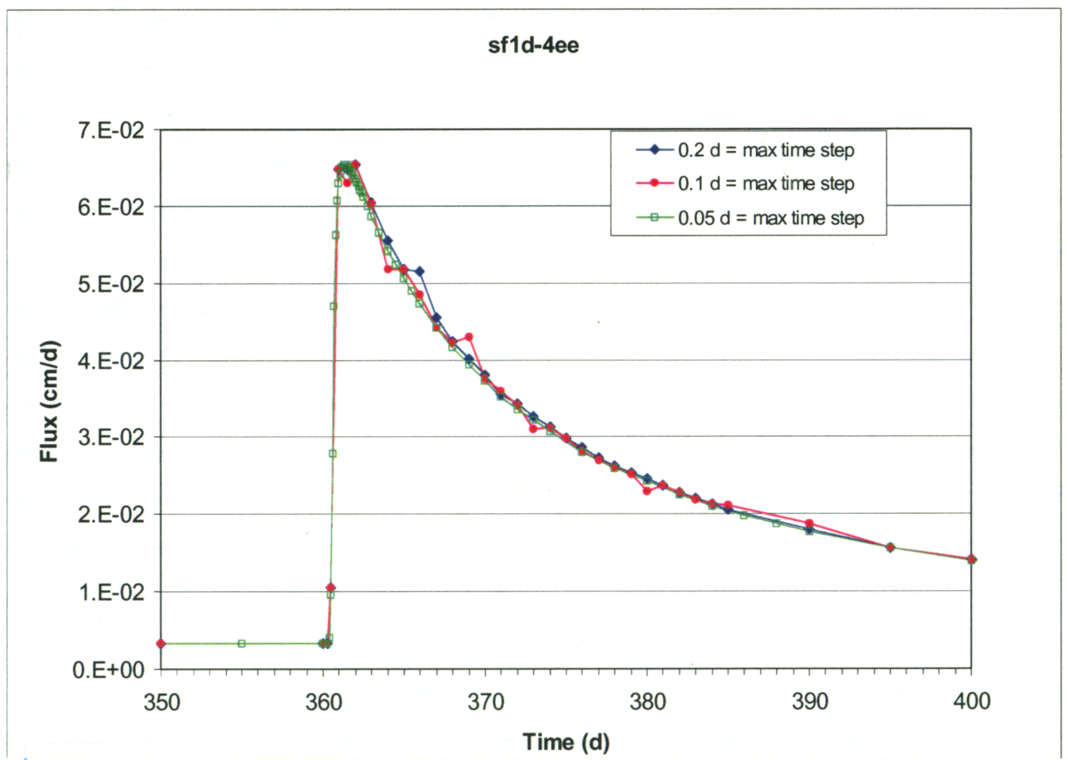

This table is a summary of the different simulations; J:\HydroProperties\Soil-Over-Fracture\runs-simulations.xls
Soil Properties, units are cm and days

		θr	θs	van Gen α	van Gen n	Ks	head	
One (%)								
sf2d-3/3a	soil	0.035	0.33	0.055	1.78	58	58	
sf2d-3/3a	bedrock	0.01	0.082	0.00012	1.69	0.0005	0.0005	Tcpmn
sf1d-3a	sf1d-3aa	0.035	0.33	0.055	1.78	0.58	0.58	wt'd avg Ks (keep soil poro and alpha)
sf1d-3b	sf1d-3bb/3	0.01025	0.08448	0.055	1.78	0.000562	0.000562	wt'd geom Ks, wt'd poro
sf1d-3c	sf1d-3cc	0.01025	0.08448	0.055	1.78	0.17	0.17	geom Ks, wt'd poro
sf1d-3d	sf1d-dd	0.01025	0.08448	0.0279	1.78	0.17	0.17	geom Ks, wt'd poro, avg alpha
sf1d-3e	sf1d-3ee	0.01025	0.08448	0.000669	1.6909	0.58	0.58	wt'd avg K, poro, alpha
sf1d-3f	sf1d-3ff	0.01025	0.08448	0.0279	1.78	58	58	wt'd avg K & poro, avg alpha
sf1d-3g	sf1d-3gg	0.01025	0.08448	0.055	1.78	0.58	0.58	wt'd avg K & poro
sf1d-3h	sf1d-3hh	0.00035	0.0033	0.055	1.78	0.58	0.58	scaled Ks and poro
sf2d-4/4a	soil	0.035	0.33	0.055	1.78	58	58	
sf2d-4/4a	bedrock	0.01	0.253	0.0008	1.84	0.33	0.33	cliff caprock, Tpcrn
sf1d-4a	sf1d-4aa	0.035	0.33	0.055	1.78	0.907	0.91	wt'd avg Ks (keep soil poro and alpha)
sf1d-4b	sf1d-4bb	0.01025	0.25377	0.055	1.78	0.348	0.348	wt'd geom Ks, wt'd poro
sf1d-4c	sf1d-4cc	0.01025	0.25377	0.055	1.78	4.375	4.375	geom Ks, wt'd poro
sf1d-4e	sf1d-4ee/2	0.00035	0.0033	0.055	1.78	0.58	0.58	scaled Ks and poro
sf1d-4f	sf1d-4ff	0.00035	0.0033	0.0279	1.78	0.58	0.58	scaled K and poro, & avg alpha
sf1d-4g	sf1d-4gg	0.00035	0.0033	0.00132	1.78	0.58	0.58	scaled K and poro, & wt'd alpha
sf1d-4h	sf1d-4hh	0.00035	0.0033	0.055	1.81	0.58	0.58	scaled K and poro, & avg n
sf1d-4i	sf1d-4ii	0.01025	0.25377	0.055	1.78	0.58	0.58	scaled K & wt'd poro
sf1d-4j	sf1d-4jj	0.01025	0.25377	0.00134	1.78	0.348	0.348	wt'd geom K, wt'd poro and alpha
sf1d-4k	sf1d-4kk	0.01025	0.25377	0.0279	1.78	0.58	0.58	scaled Ks, wt'd poro, and avg alpha
sf1d-4m	sf1d-4mm	0.01025	0.25377	0.055	1.78	0.91	0.91	wt'd avg Ks, poro
sf1d-4n	sf1d-4nn	0.01025	0.25377	0.0279	1.78	0.91	0.91	wt'd avg Ks, poro, & avg alpha
sf1d-4o	sf1d-4oo	0.01025	0.25377	0.00132	1.78	0.91	0.91	wt'd avg Ks, poro, & wt'd alpha
Ten (%)								
sf2d-5/5a	soil	0.035	0.33	0.055	1.78	58	58	
sf2d-5/5a	bedrock	0.01	0.253	0.0008	1.84	0.33	0.33	cliff caprock, Tpcrn
sf1-5	sf1-5a	0.0125	0.2607	0.0062	1.78	6.1	6.1	wt'd avg poro, Ks, alpha
sf1-5b	sf1-5bb	0.0125	0.2607	0.055	1.78	6.1	6.1	wt'd avg poro, Ks
sf1-5c	sf1-5cc	0.0125	0.2607	0.055	1.78	0.553	0.553	wt'd avg poro, wt'd geom Ks
sf1-5d	sf1-5dd	0.0125	0.2607	0.0062	1.78	0.553	0.553	wt'd avg poro and alpha, wt'd geom Ks
sf1-5e	sf1-5ee	0.0035	0.033	0.055	1.78	5.8	5.8	scaled poro, Ks
sf1-5f	sf1-5ff	0.0125	0.2607	0.05	1.78	6.1	6.1	wt'd avg poro, Ks, reverse wt'd alpha
sf2d-7/7a	soil	0.035	0.33	0.055	1.78	58	58	
sf2d-7/7a	bedrock	0.01	0.082	0.00012	1.69	0.0005	0.0005	Tcpmn
sf1d-7a	sf1d-7aa	0.0125	0.1068	0.055	1.78	5.8	5.8	wt'd avg poro, Ks
sf1d-7b	sf1d-7bb	0.0125	0.1068	0.0056	1.78	5.8	5.8	wt'd avg poro, Ks, alpha
sf1d-7c	sf1d-7cc	0.0125	0.1068	0.055	1.78	0.0016	0.0016	wt'd avg poro, wt'd geom Ks
sf1d-7d	sf1d-7dd	0.0125	0.1068	0.055	1.78	0.17	0.17	wt'd avg poro, geom Ks

Initial conditions for 10% and 1% 2D simulations in terms of water content (sf2d-7a and sf2d-3a). These graphs of (below) illustrate why the pulse arrives at the bottom sooner in the 1% case; this is because the fracture is wetter in the 1% case. Remember that a uniform influx of 12 mm/yr is applied to get the initial conditions. At a lower influx rate, the 1% fracture saturation would be lower. This means that the 1% fracture case cannot drain the pulse with the initial condition of 12mm/yr infiltration given the K_{sat} and unsaturated properties of the soil.

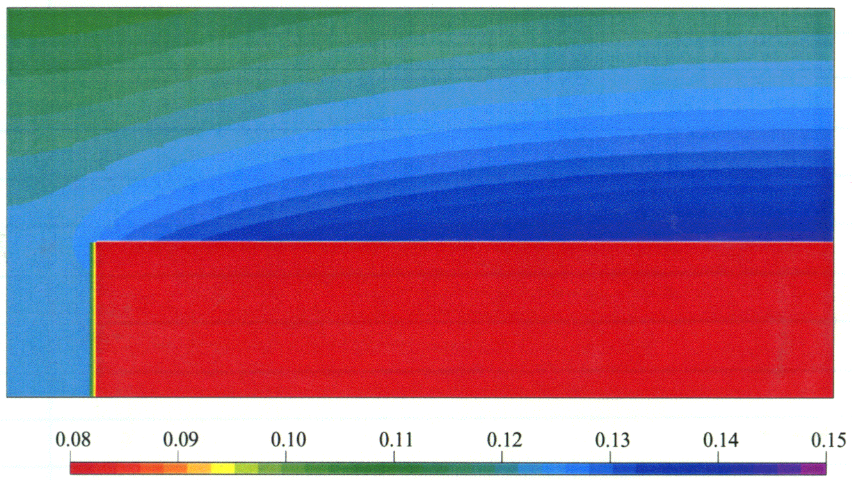

water content 10 % fracture case

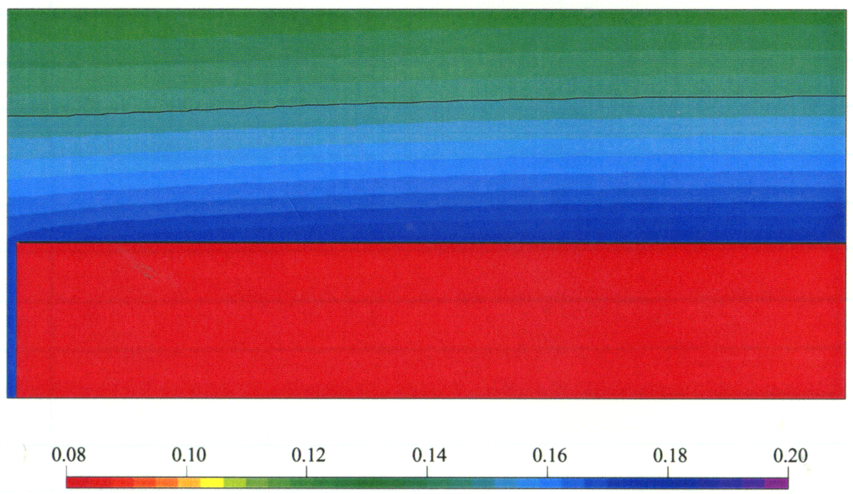

water content 1 % fracture case

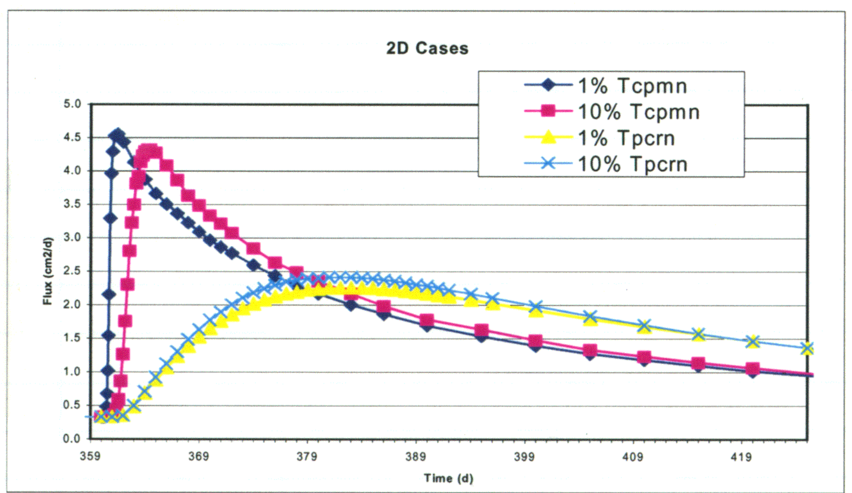

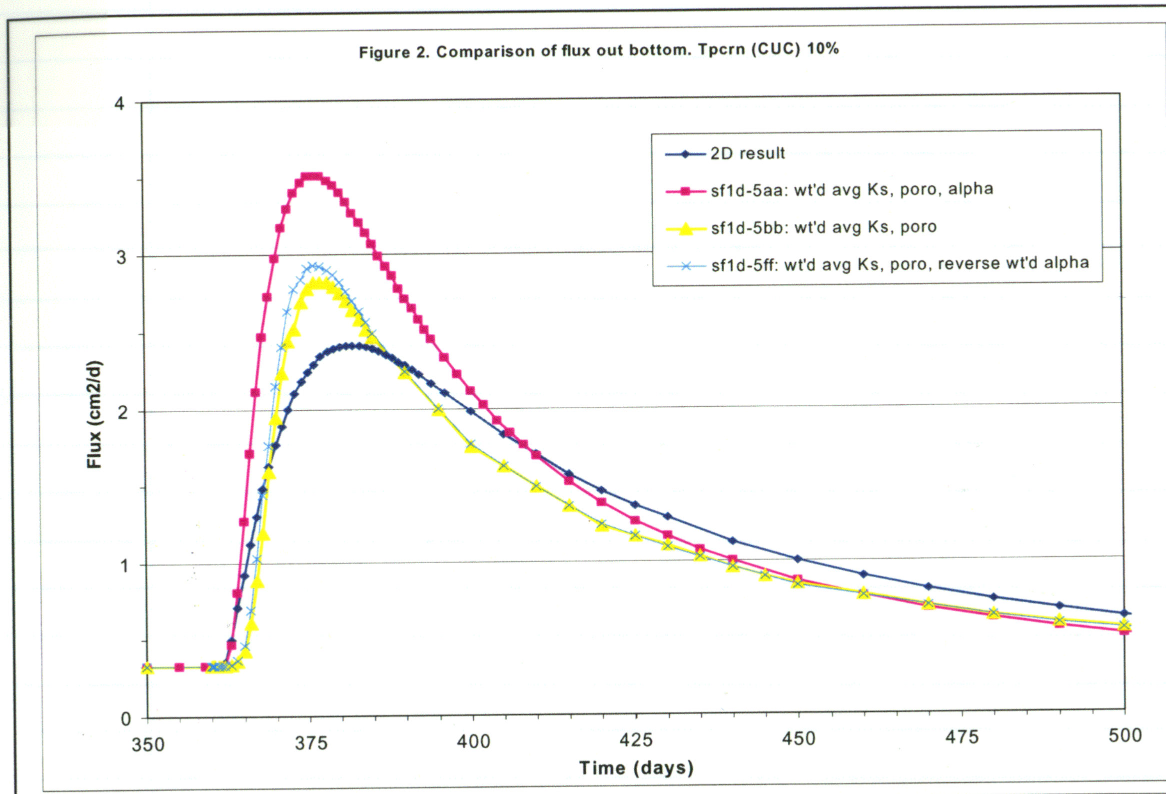

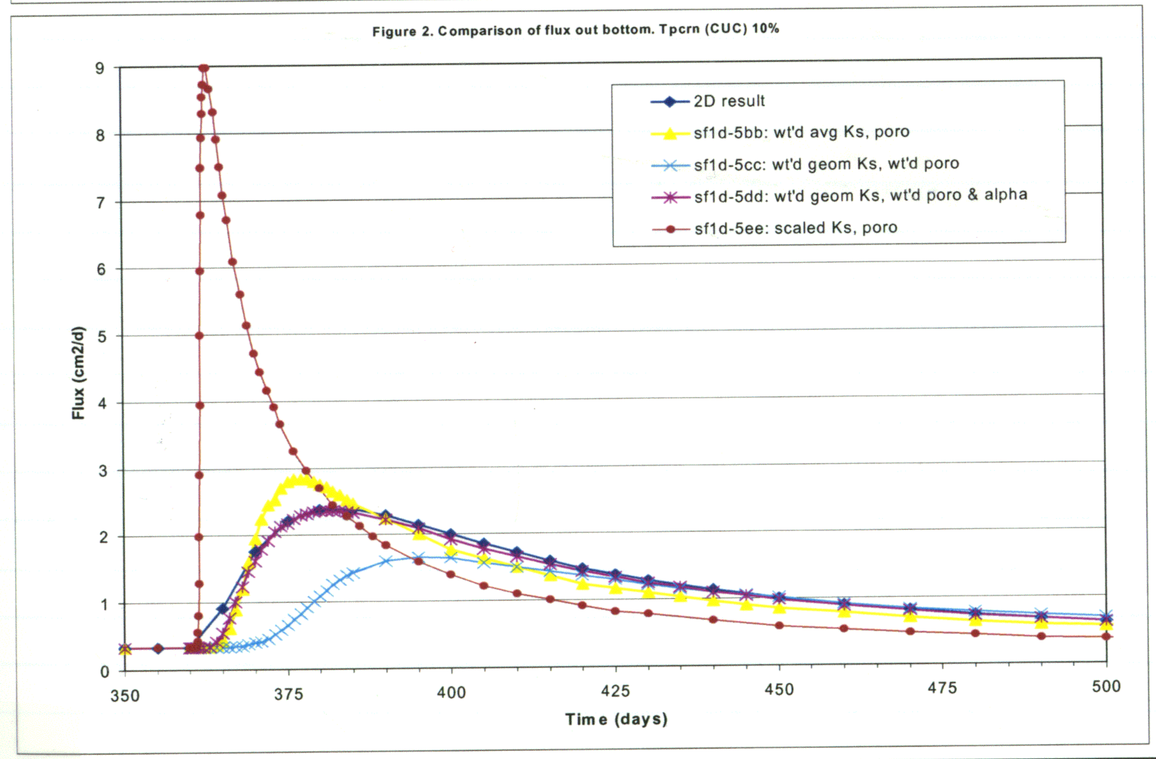

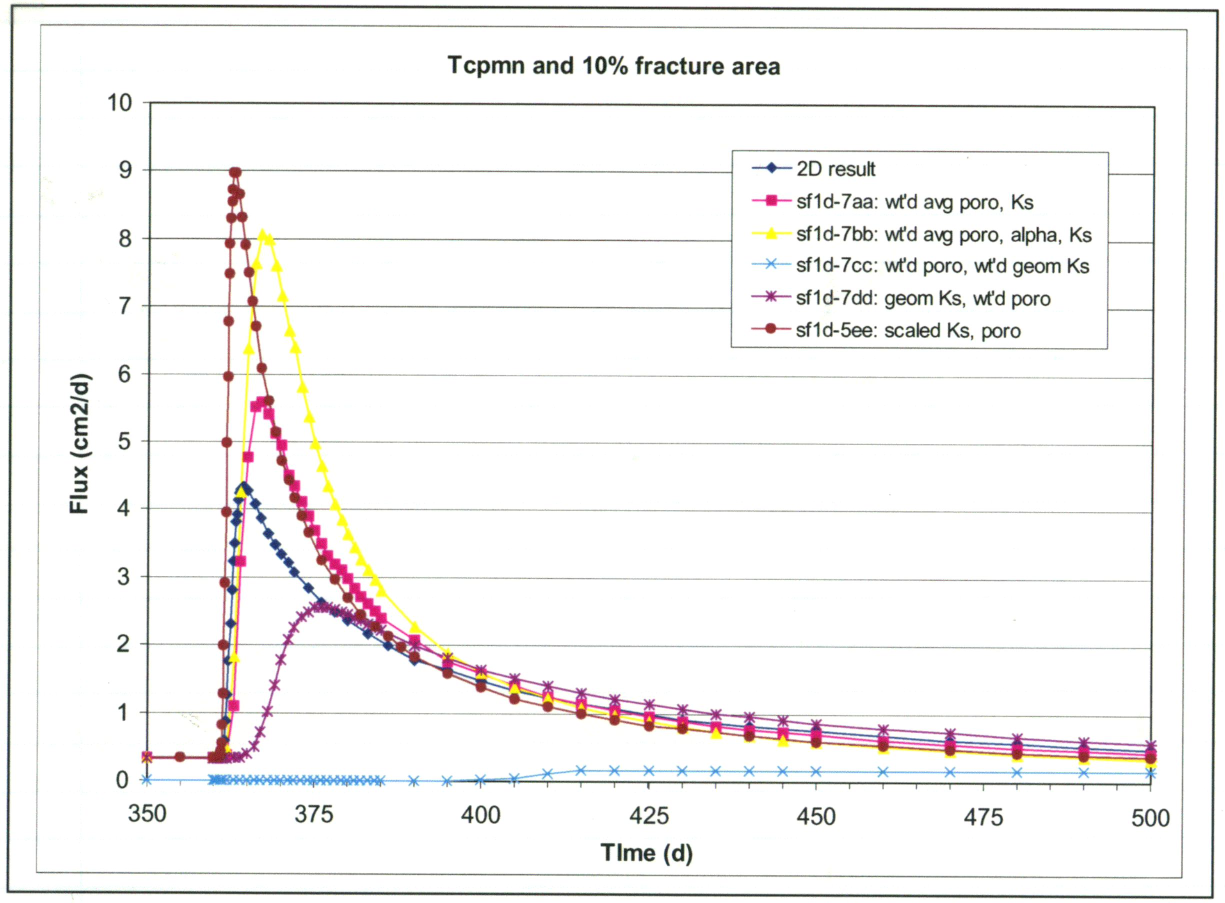
Tcpmn and 10% fracture area
2D result
sf1d-7aa: wt'd avg poro, Ks
sf1d-7bb: wt'd avg poro, alpha, Ks
sf1d-7cc: wt'd poro, wt'd geom Ks
sf1d-7dd: geom Ks, wt'd poro
sf1d-5ee: scaled Ks, poro
Flux (cm2/d)
0
1
2
3
4
5
6
7
8
9
10
350
375
400
425
450
475
500
TIme (d)

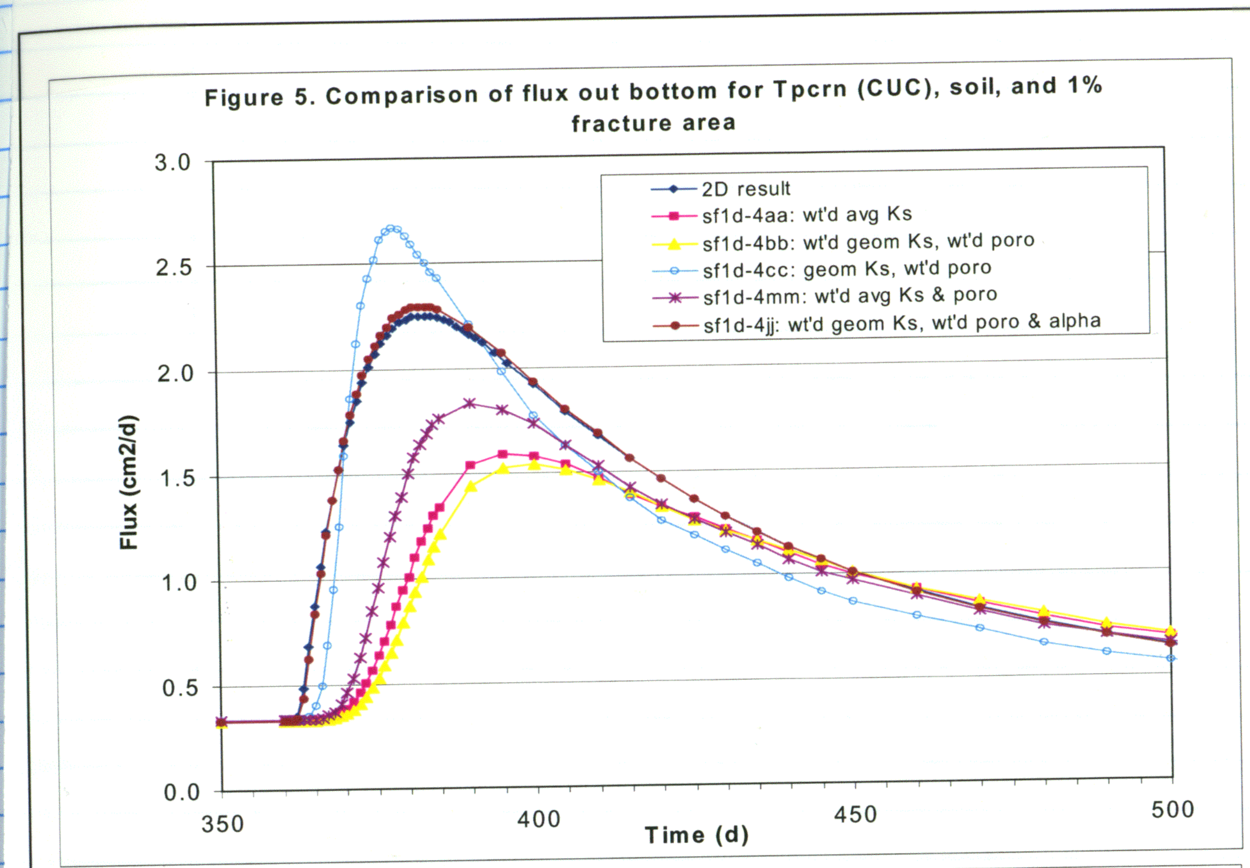
Figure 5. Comparison of flux out bottom for Tpcrn (CUC), soil, and 1% fracture area
2D result
sf1d-4aa: wt'd avg Ks
sf1d-4bb: wt'd geom Ks, wt'd poro
sf1d-4cc: geom Ks, wt'd poro
sf1d-4mm: wt'd avg Ks & poro
sf1d-4jj: wt'd geom Ks, wt'd poro & alpha
Flux (cm2/d)
0.0
0.5
1.0
1.5
2.0
2.5
3.0
350
400
450
500
Time (d)

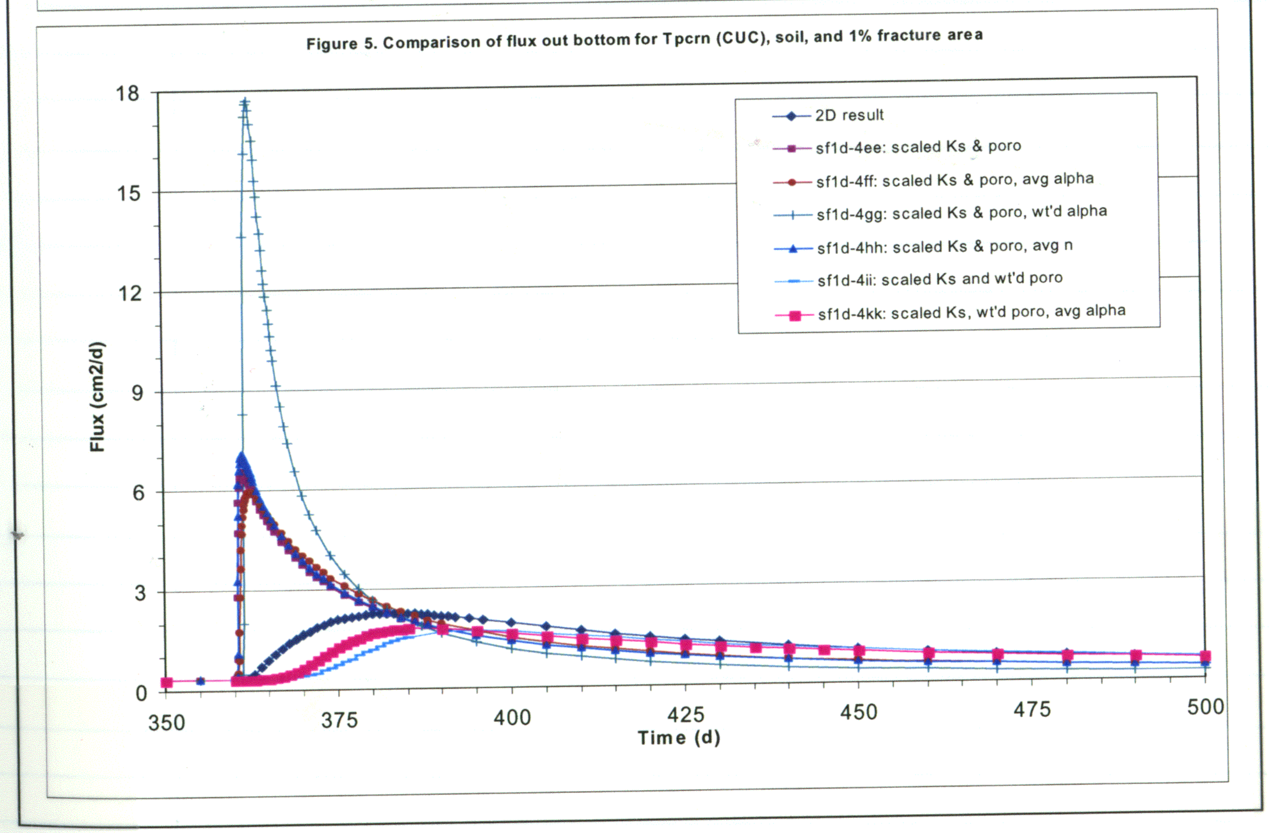
Figure 5. Comparison of flux out bottom for Tpcrn (CUC), soil, and 1% fracture area
2D result
sf1d-4ee: scaled Ks & poro
sf1d-4ff: scaled Ks & poro, avg alpha
sf1d-4gg: scaled Ks & poro, wt'd alpha
sf1d-4hh: scaled Ks & poro, avg n
sf1d-4ii: scaled Ks and wt'd poro
sf1d-4kk: scaled Ks, wt'd poro, avg alpha
Flux (cm2/d)
0
3
6
9
12
15
18
350
375
400
425
450
475
500
Time (d)

Figure 5. Comparison of flux out bottom for Tpcrn (CUC), soil, and 1% fracture area

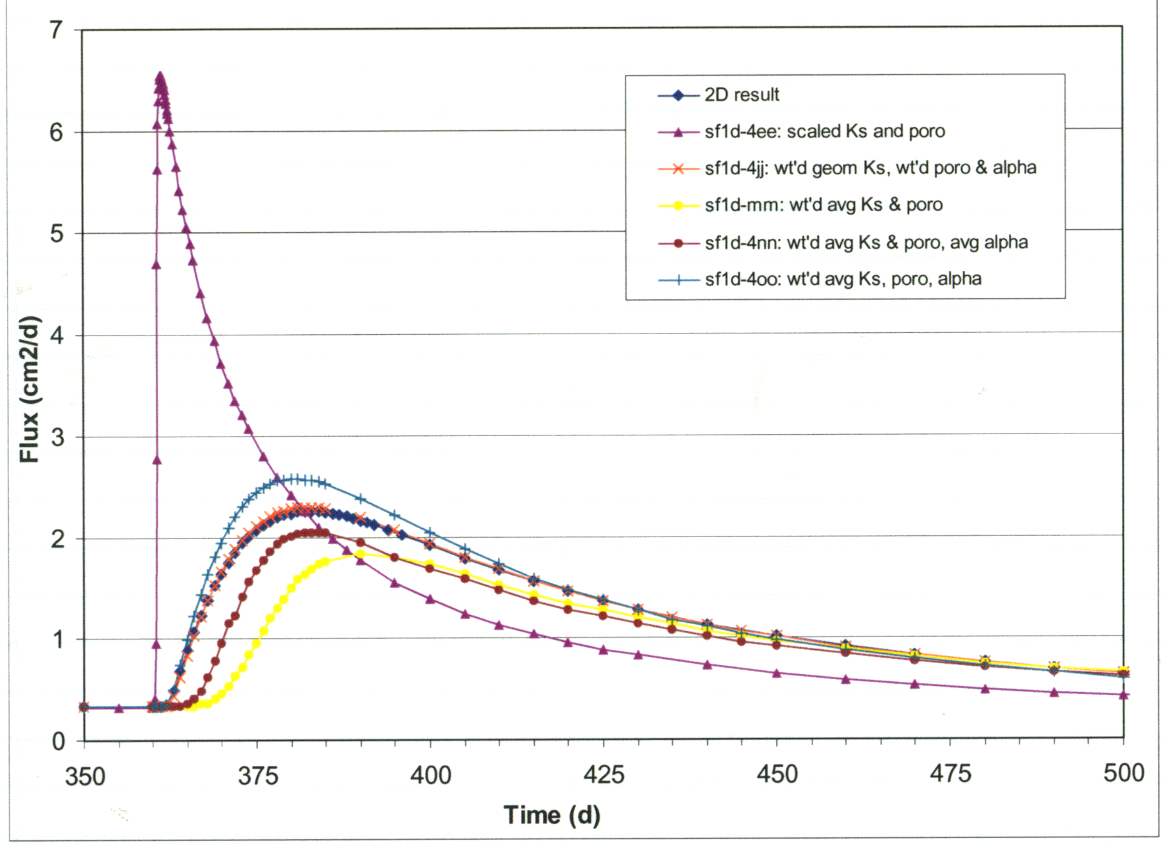

Figure 6. Comparison of flux out bottom for Tcpmn, soil, and 1% fracture area

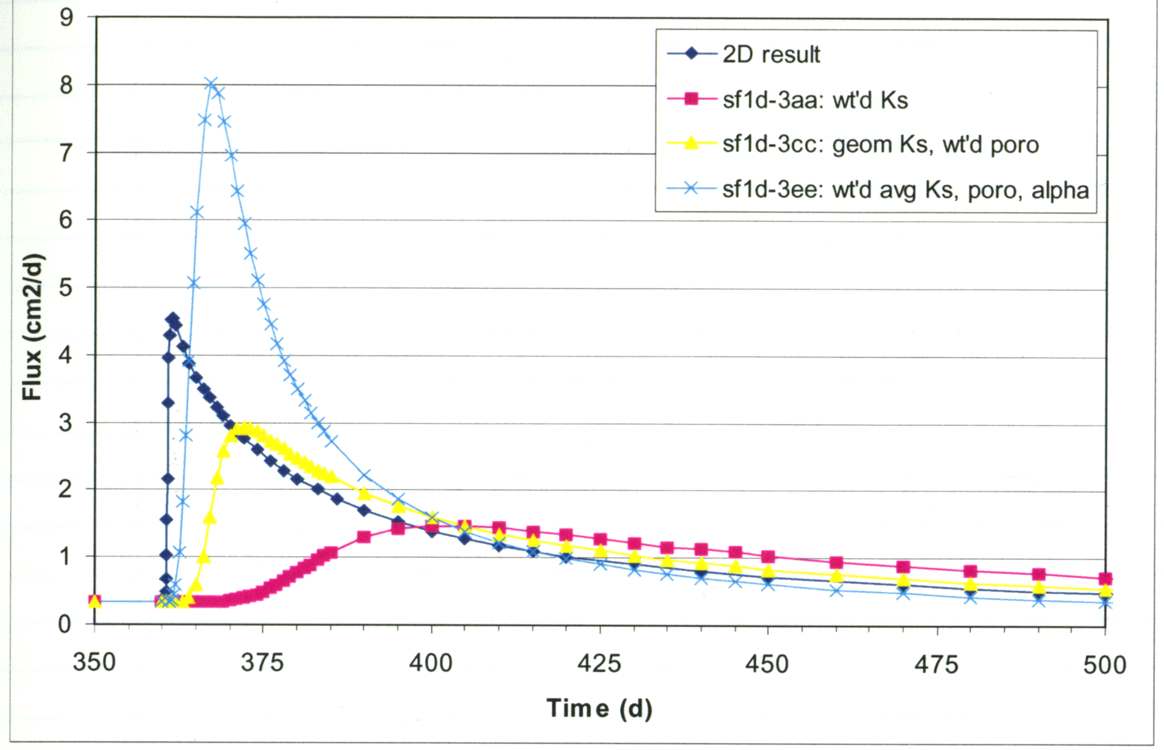

Figure 6. Comparison of flux out bottom for Tcpmn, soil, and 1% fracture area

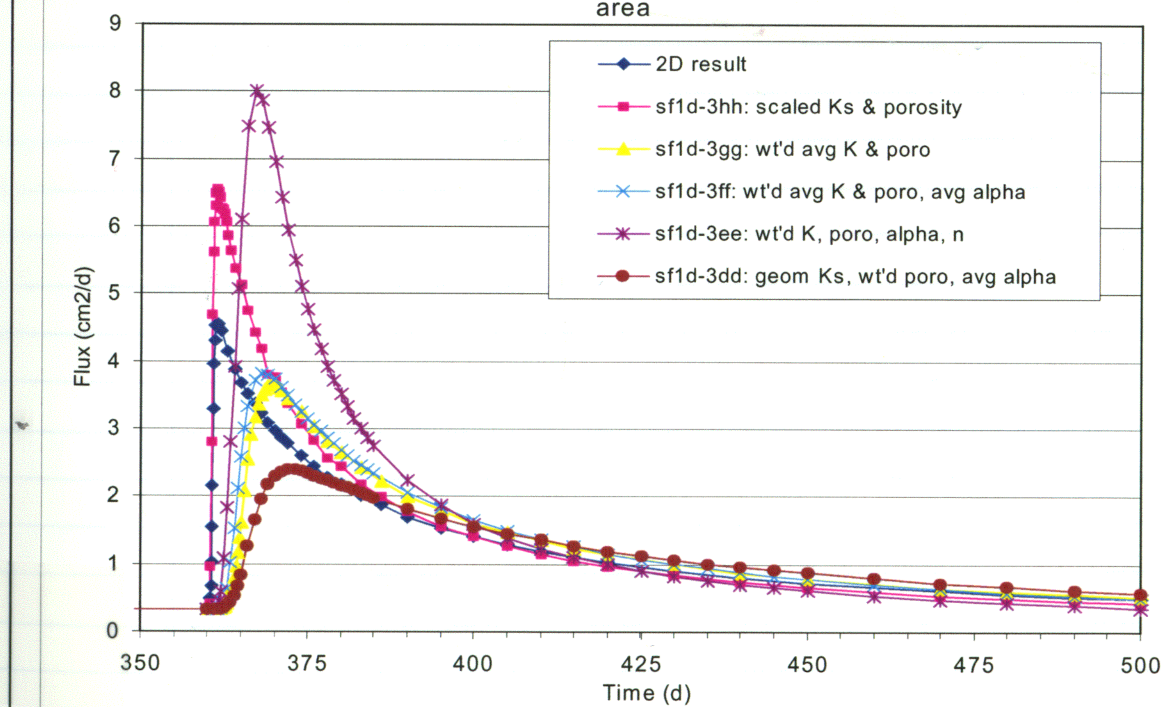

Discussion

Initial conditions play a big part in controlling the timing of the pulse (and I used the steady state rate to control the initial conditions). If conditions are wetter at start of pulse, then ….
If conditions are drier at start of pulse, then ….
The blip is for real, initially, the effective permeability of the bedrock is greater than that for the soil in the fracture. Once the pressure has risen enough, the reverse comes to be (effective K of soil becomes greater than that for the bedrock). Note that we are modeling in the region surrounding the crossover point of the effective conductivity curves plotted in an earlier figure. Also note that the magnitude of the pulse coming out the bottom for the 1.2 mm/yr case shown below is much lower than the pulse for the higher initial condition (greater steady state flux of 12 mm/yr)

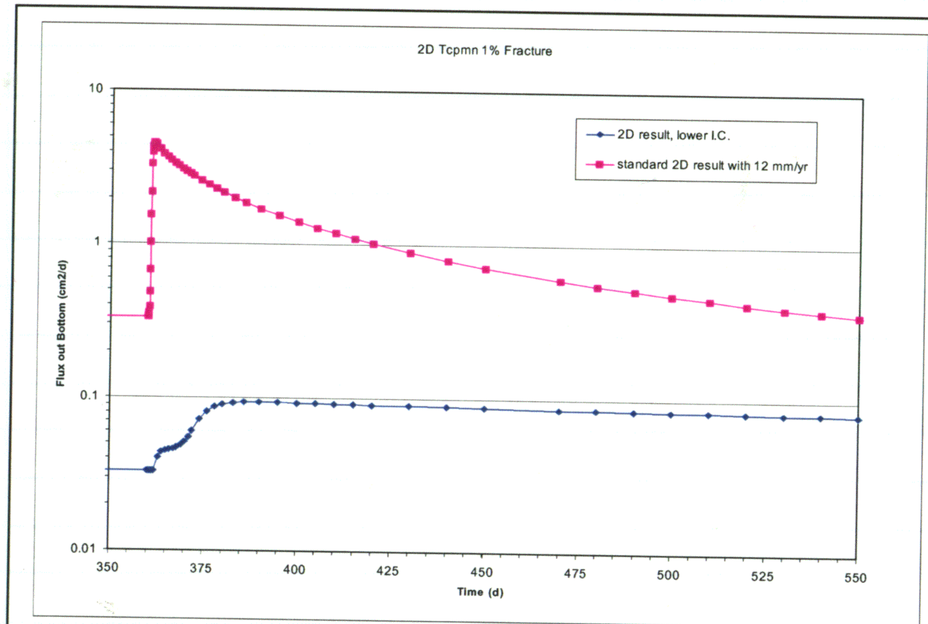

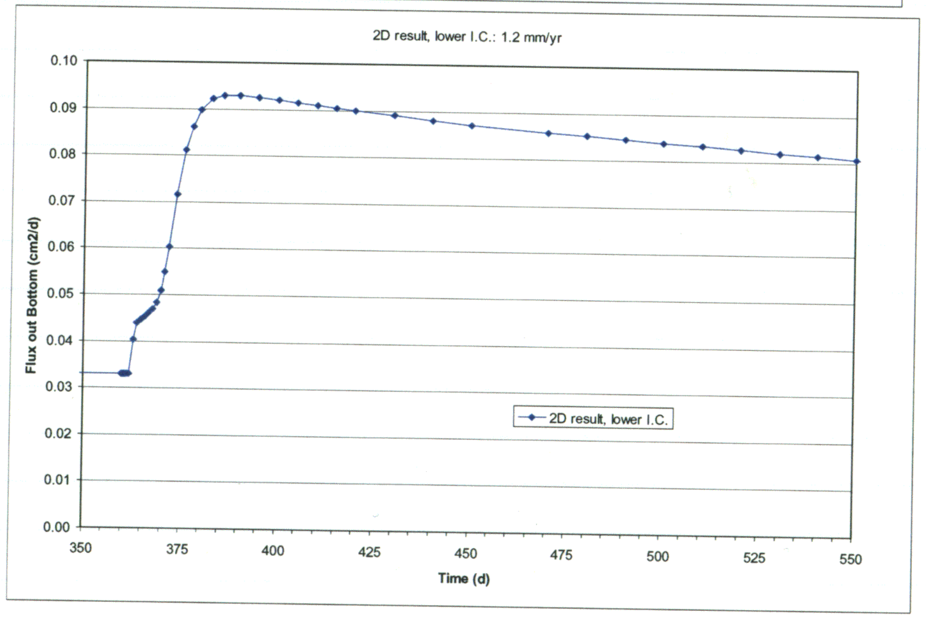

Some pertinent comments that may be addressed in later work:

1. The effect of soil depth was not considered here (a 30 cm thick soil column reflective of typical conditions over the repository).

2. The effect of fracture percentage may have to be explored further. The 10% case is not realistic and definitely exhibited different flow characteristics as compared to the 1% case. Maybe simulations of another small fracture porosity are warranted. There may also be an effect of the difference between the bedrock and soil permeabilities combined with the magnitude of the fracture area (porosity).

3. The effect of soil properties was not addressed. Variations in the soil properties may affect the flow characteristics (the interaction between the soil in the fracture and the bedrock matrix).

4. The effect of bedrock properties is addressed below for the original soil property and fracture porosities, but may have to be analyzed further for different initial conditions, soil properties, and fracture porosities.

Methodology for Determining Which Averaging Scheme

There is some point at which the scaling procedure falls down. It works acceptably when the bedrock matrix can be considered impermeable. But as the bedrock K_{sat} gets to within a couple orders of magnitude of the fracture fill material (soil, as assumed here), the bedrock hydrologic properties dominate the control over flow in the shallow infiltration environment.

To determine the point at which the bedrock properties begin to exert control over the flow environment, the Tpcmn and Tpcrn (caprock cliff former) simulations were re-run so that a sum of the square of the differences (SSD) between the 2D and 1D simulated flows out the bottom of the domain could be calculated. The 2D and all of the 1D simulations must be run using the same output times. I switched to a 50 day total simulation with the pulse into the top of the domain occurring at 0.05 to 0.099 days. In HYDRUS2D, there is no way to start the simulation with a non-zero specified flux on the top at time 0; hence, there is a slight blip as the specified flux of 12 mm/yr is not fully in place until 0.001 days (HYDRUS2D ramps the specified fluxes, instead of discrete jumps). This blip is considered minor and does not affect results. This was done using the same file names but copied to a new directory so that the original outputs could be retained:
J:\Hydrus2d\Differences-OneTen*

To illustrate the transition, SSD for each type of averaging will be plotted against some variable that is based on bedrock permeability. The difference between the soil permeability and the bedrock permeability in log space is deemed the most useful: $\Delta[\log(K_{sat})]$. In order to create plots illustrating the transition, another material was simulated so that 3 points make up a line instead of just 2 points (Tpcmn and Tpcrn are already simulated). The caprock (TC) unit labeled as Tpcrv in Flint et al. (1996) fills in the middle ground in terms of permeability; this zone is also called CCR in Flint (1998). Note that Tpcrn (CUC) is the upper cliff in the nonlithophysal zone of the crystal-rich member; the Tpcrv is the vitric zone of the crystal-rich member and it overlies the Tpcrn. There are only areas of vitric caprock on YM, most of the broad slope at the YM crest is part of the nonlithophysal zone Tpcrn (Tcr1, Tcr2, Tcr3 in the nomenclature of Day et al. 1998).

The properties of the Tpcrv used in the simulations sf2d-9a, sf1d-9aa, sf1d-9cc (sf1d-4ee is still relevant for the scaled parameter result) are shown in the table on the top of the following page; the soil properties are the same as before:

	Tpcrv	sf1d-9aa 1% wt'd avg Ks & ϕ	sf1d-9cc 1% wt'd geom Ks, wt'd ϕ & α	Flint et al 1996Table 2	Flint Units
Ks cm/d	0.014	0.594	0.015	0.138	mm/d
ϕ	0.048	0.051	0.051	0.048	
θ r	0.01	0.01025	0.01025	0.01	
α cm-1	8.7E-04	.055	1.4E-03	0.885	bar-1
van Gen n	1.24	1.78	1.78	1.24	

To further fill in the gap along the curve, I simulated the Tptpll (lower lithophysal of the Topopah Springs welded; its properties lie between the Tpcrv and the Tpcmn of the Tiva Canyon. The properties of the Tptpll used in the simulations sf2d-8a, sf1d-8aa, sf1d-8cc, and sf1d-8dd (sf1d-4ee is still relevant for the scaled parameter result) are shown in the table below

	Tptpll	sf1d-8aa 1% wt'd avg Ks & ϕ	sf1d-8cc 1% wt'd geom Ks,wt'd ϕ & α	Flint et al 1996Table 2	Flint Units
Ks cm/d	0.002	0.582	0.0022	0.02	mm/d
ϕ	0.13	0.132	0.132	0.13	
θ r	0.01	0.01025	0.01025	0.01	
α cm-1	2.7E-04	0.055	8.2E-04	0.273	bar-1
van Gen n	1.294	1.78	1.78	1.294	

	Unit 1	sf1d-6aa 1% wt'd avg Ks & ϕ	sf1d-6cc 1% wt'd geom Ks, wt'd ϕ & α	Synthetic Data	units
Ks cm/d	0.0065	0.586	0.0071	0.065	mm/d
ϕ	0.17	0.172	0.172	0.17	
θ r	0.01	0.01025	0.01025	0.01	
α cm-1	5.9E-04	0.055	1.1E-03	0.6	bar-1
van Gen n	1.5	1.78	1.78	1.5	

All of the simulation results (flux out the bottom) for these last 3 series of problems are pasted into :
J:\HydroProperties\Soil-Over-Fractures\simulations.xls in worksheet "Differences"

The qualitative observations from the plots of flux out the bottom (shapes of pulse, timing of pulse) are supported by the sum of the squares of the differences plots.

The results are plotted in the figures on the following page.

Pages 70-105 taped in 9/28/00 RF

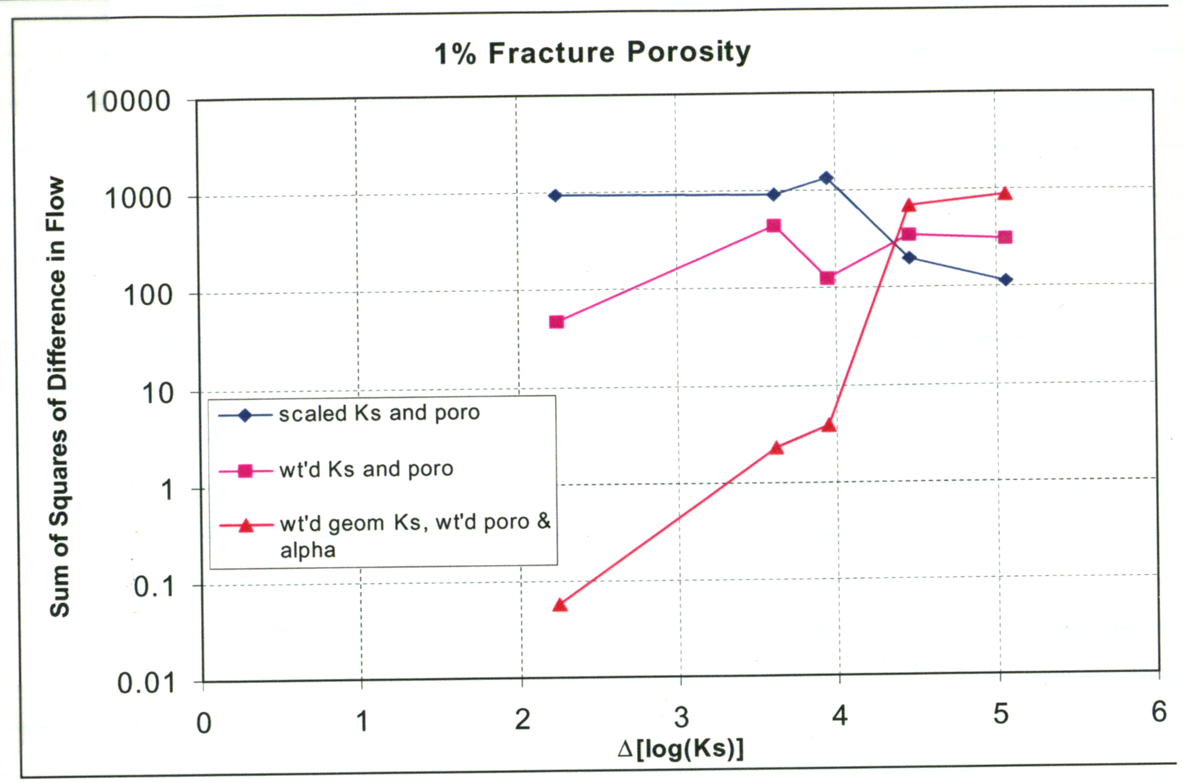

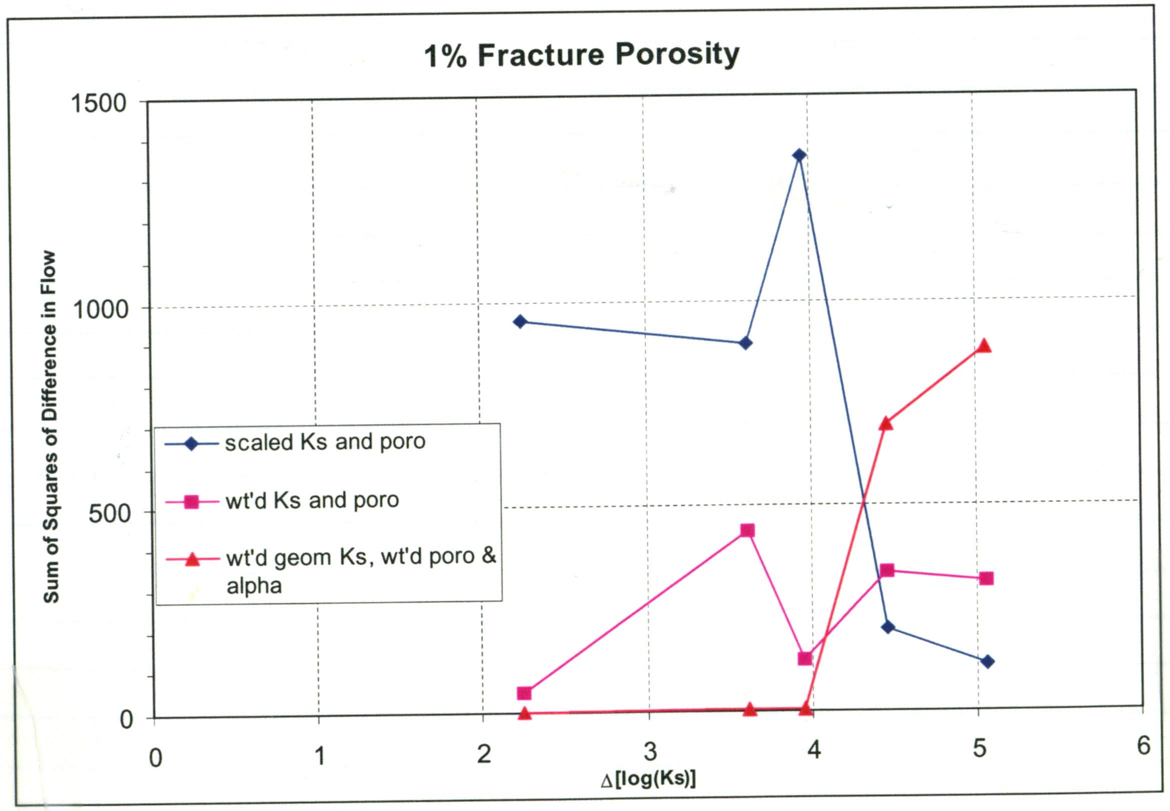

Last entry 9/28/00 RF

I HAVE reviewed this notebook. It appears to adequately comply with QAP-001. Specifically, as required by QAP-001, but for the record, there appears to be adequate information here for another, qualified, person to reproduce the work.

E. C. Perry
10/11/2000

page 2. bren: ~/Watershed/
bubo: d:\AvData\clr_blk\

page 15. bubo: d:\Randy\Wodhiser\SpeitWash\

page 24. bubo: d:\AVData\WDay\

page 26. bubo: d:\AVData\Soils\

page 27. bubo: d:\AVData\Dog\

pages 29-39 bren: ~/soilDepthTPA/
bren: ~/SoilDepthStu/
bubo: D:\AVData\WatershedGrid\

page 40 bubo: D:\Randy\Soils\
bubo: D:\AVData\YM\

page 47-52 bubo: D:\AVData\WatershedGrid\
bubo: D:\AVData\Dog\
bubo: D:\AVData\WDay\cb\
bubo: D:\Randy\Wodhiser\SpeitWash\Photos

page 58-60 bubo: D:\AVData\Repository*

page 60- bubo: J:\AVData\Green\

page 70-77 } put onto 2 cdroms
page 78-105 } includes J:\AVData\WatershedGrid*

ADDITIONAL INFORMATION FOR SCIENTIFIC NOTEBOOK #: 294

Document Date:	10/12/1998
Availability:	Southwest Research Institute® Center for Nuclear Waste Regulatory Analyses 6220 Culebra Road San Antonio, Texas 78228
Contact:	Southwest Research Institute® Center for Nuclear Waste Regulatory Analyses 6220 Culebra Road San Antonio, TX 78228-5166 Attn.: Director of Administration 210.522.5054
Data Sensitivity:	■"Non-Sensitive" □ Sensitive □"Non-Sensitive - Copyright" □ Sensitive - Copyright
Date Generated:	10/21/1999 through 10/02/2000
Operating System: (including version number)	Windows
Application Used: (including version number)	Microsoft NT
Media Type: (CDs, 3 1/2, 5 1/4 disks, etc.)	6 CDs
File Types: (.exe, .bat, .zip, etc.)	apr, dbf, shx, shp, ps, eps, dat, dos, cgi, txt, xls, bmp, jpg
Remarks: (computer runs, etc.)	Media contains: Watershed Modeling; Solitario Canyon-Splitwash